Geosci. Model Dev. Discuss., 5, 2347–2443, 2012
www.geosci-model-dev-discuss.net/5/2347/2012/
doi:10.5194/gmdd-5-2347-2012

Geoscientific Model Development Discussions

SPITFIRE-2: an improved fire module for Dynamic Global Vegetation Models

M. Pfeiffer and J. O. Kaplan

ARVE Group, Ecole Polytechnique Fédérale de Lausanne, Switzerland

Received: 8 August 2012 – Accepted: 10 August 2012 – Published: 23 August 2012

Correspondence to: M. Pfeiffer (mirjam.pfeiffer@epfl.ch)

Published by Copernicus Publications on behalf of the European Geosciences Union.

Abstract

Fire is the primary disturbance factor in many terrestrial ecosystems. Wildfire alters vegetation structure and composition, affects carbon storage and biogeochemical cycling, and results in the release of climatically relevant trace gases, including CO_2, CO, CH_4, NO_x, and aerosols. Assessing the impacts of global wildfire on centennial to multi-millennial timescales requires the linkage of process-based fire modeling with vegetation modeling using Dynamic Global Vegetation Models (DGVMs). Here we present a new fire module, SPITFIRE-2, and an update to the LPJ-DGVM that includes major improvements to the way in which fire occurrence, behavior, and the effect of fire on vegetation is simulated. The new fire module includes explicit calculation of natural ignitions, the representation of multi-day burning and coalescence of fires and the calculation of rates of spread in different vegetation types, as well as a simple scheme to model crown fires. We describe a new representation of anthropogenic biomass burning under preindustrial conditions that distinguishes the way in which the relationship between humans and fire are different between hunter-gatherers, obligate pastoralists, and farmers. Where and when available, we evaluate our model simulations against remote-sensing based estimates of burned area. While wildfire in much of the modern world is largely influenced by anthropogenic suppression and ignitions, in those parts of the world where natural fire is still the dominant process, e.g. in remote areas of the boreal forest, our results demonstrate a significant improvement in simulated burned area over previous models. With its unique properties of being able to simulate preindustrial fire, the new module we present here is particularly well suited for the investigation of climate-human-fire relationships on multi-millennial timescales.

1 Introduction

Fire is one of the most important disturbance processes that affect the terrestrial biosphere. Wildfires alter vegetation composition, structure and distribution, biomass

GMDD
5, 2347–2443, 2012

productivity, plant diversity and biogeochemical cycles (Johnson et al., 1998; Moreira, 2000; Ojima et al., 1994; Wan et al., 2001; Neary et al., 2005; Bond et al., 2005). Understanding the causes and consequences of wildfire is critical for Earth system modeling due to its close coupling with vegetation and climate (Bowman et al., 2009). Biomass burning is a key process controlling the spatial and interannual variability in the emissions of climatically relevant trace gases, including CO_2, CO, CH_4 and NO_x (Crutzen and Andreae, 1990; Penner et al., 1992; Andreae and Merlet, 2001; Jain et al., 2006). As natural and human-caused fires affect most ecosystems from tropical forests to tundra (Bond and van Wilgen, 1996; Dwyer et al., 2000), changes in biomass burning over long timescales, e.g. throughout the Holocene, are likely to have affected both the global carbon budget and the distribution of plants on Earth at the present (Pausas and Keeley, 2009). For example, industrial fire suppression that started in the early 20th century (see, e.g. Pyne, 1982, Fig. 1; Keeley et al., 1999; Houghton et al., 2000) has significantly modified the structure and composition of many terrestrial ecosystems with concomitant changes in biogeochemical and hydrologic cycling (Grimm, 1984; Clark, 1990; Belillas and Rodà, 1993; Busch and Smith, 1993; Moreira, 2000; Tilman et al., 2000; Shu-ren, 2003; Foster et al., 2003; Mouillot et al., 2006; Sundarambal et al., 2010). These changes have occurred over large enough spatial scale and so rapidly so as to have potentially affected regional climate, water cycling and quality, and carbon budgets (Fahenstock and Agee, 1983; Andreae, 1991; Stocks, 1991; Dixon et al., 1994; Sohngen and Haynes, 1997; Tilman et al., 2000; Shu-ren, 2003; Cerdà and Doerr, 2005). Likewise, human activities over the 11 millennia of the preindustrial Holocene probably had substantial influences on terrestrial ecosystems and our perception of what constitutes "natural" terrestrial ecosystems (Pyne, 1994; Head, 1994; Pyne, 1997; Carcaillet, 1998; Williams, 2000; Kimmerer and Lake, 2001; Carcaillet et al., 2002; Stewart et al., 2002; Ruddiman, 2007; Boyd, 2002).

Recently, synthesis of archives of charcoal records from lake sediments and other terrestrial archives (Anshari et al., 2001; Haberle and Ledru, 2001; Whitlock and Larsen, 2002; Gavin et al., 2003; Lynch et al., 2004a; Bush et al., 2007; Marlon et al.,

GMDD
5, 2347–2443, 2012

2008; Power et al., 2008, 2010) has led to a qualitative estimation of the time trend and roughly millennial-scale variability in global biomass burning over the terminal Pleistocene and Holocene. While extensive, the current version of the Global Charcoal Database is characterized by a considerable spatial heterogeneity in sample site distribution with certain parts of the world being less well represented than others, therefore being unable to provide an adequate and qualitatively comparable spatio-temporal coverage for all regions at the same time. Power et al. (2008) state that the interpretations of the spatial and temporal patterns of change in fire regimes deduced from the global charcoal database can be regarded as hypotheses, but nevertheless require rigorous testing at global and regional scales. Inter-site comparability is further complicated by the variety of different record types and site types (e.g. macroscopic and microscopic charcoal, from lakes, mires or alluvial-fan sediment records, sampled as particle counts, weight or volume of charcoal per unit sediment) with varying temporal resolution and dating control (Power et al., 2008). Low temporal resolution of charcoal records leaves open questions as to changes in fire regimes that may not be reflected by the records. For smaller regions, synthesis of high-resolution charcoal records has enabled the development of a clearer picture of the relationship between humans, climate, and fire at roughly centennial scale (e.g. see Long et al., 1998; Vannière et al., 2008; Rius et al., 2012).

However, global-scale quantification of natural and anthropogenic burning on long time scales is not possible based on proxy records alone. For example, synthesis of charcoal records from multiple sites is generally limited to estimates of fire frequency and precludes the ability to estimate fire intensity or burned area, both of which would be required to estimate trace gas and aerosol emissions. Thus, to build a picture of wildfire activity in the past that is quantitative and spatially and temporally coherent, and to quantify fire effects on vegetation, carbon pools and trace gas emissions, requires the development and application of models of fire dynamics coupled with general vegetation dynamics.

GMDD
5, 2347–2443, 2012

Process-based modeling of fire in the terrestrial biosphere is challenging as it involves a variety of different factors that need to be determined correctly in order to be able to simulate impacts of biomass burning as accurately as possible. Vegetation and fire are both influenced by climate and human activities, but conversely vegetation will also influence fire behavior via its structure, fuel load and fuel quality. At the same time, fire alters vegetation composition and structure, which implies that both positive and negative feedback mechanisms are likely to develop over time that balance vegetation dynamics and fire against one other. At continental to global scales, climate and vegetation influence the occurrence of fire by affecting fuel load, fuel quality and flammability and fire spread (Archibald et al., 2009), and fire in return shapes vegetation composition and structure and influences climate directly through emissions of climatically relevant trace gases, and indirectly by altering vegetation characteristics that determine albedo, surface roughness and fluxes of water, energy and momentum. It is therefore essential to have a good combined representation of both vegetation and fire dynamics in any model that simulates the role of fire in the Earth System.

Mathematical models of wildfire dynamics have been under development for more than 40 yr (Rothermel, 1972). The original attempts to model fire behavior were motivated by needs for operational forecasting for firefighting and forest management applications. These models were applied at relatively small spatial scales of 10^0–10^3 ha, and have been extensively revised and updated over subsequent years (Burgan and Rothermel, 1984; Andrews, 1986, 2007; Burgan, 1987; Andrews and Chase, 1989; Reinhardt et al., 1997; Finney, 1998; Andrews et al., 2003, 2008; Heinsch and Andrews, 2010). Fire modeling at field scale is an essential part of fire management and mitigation worldwide, and modern operational fire models such as BehavePlus 5.0 can be used for a host of fire management applications, including projecting the behavior of ongoing fire, planning prescribed fire, assessing fuel-hazard, and training (Heinsch and Andrews, 2010).

More recently, fire models have been developed for application at larger spatial scales, e.g. for integration into DGVMs in order to simulate the fundamental disturbance

GMDD
5, 2347–2443, 2012

process that fire represents, and in some cases to estimate the emissions of climate-relevant trace gases and aerosols at continental to global scale. Depending on the goals for application of the particular DGVM, the detail with which fire is represented varies, but all fire modules include a representation of three key processes:

1. fire occurence
2. fire spread
3. fire impact

The most simple type of fire modules incorporated into DGVMs include those used in TRIFFID (Cox, 2001), SDGVM (Woodward and Lomas, 2004), IBIS (Kucharik et al., 2000), ED (Moorcroft et al., 2001) or VEGAS-DGVM (Zeng et al., 2005). These models either represent all disturbances, including fire, as a time-invariant loss rate, or parameterize fire as a simple empirical function of litter moisture and quantity. As none of these simple schemes take into account potential interactions and feedbacks between vegetation and fire, none of them are suitable to assess the changing role of fire linked to changes in climate or human impact.

In comparison with these simple representations, fire models of intermediate complexity can represent the major processes of vegetation-fire dynamics while being computationally inexpensive. These models include Glob-FIRM (Thonicke et al., 2001), Reg-FIRM (Venevsky et al., 2002), and CTEM-FIRE (Arora and Boer, 2005) and have been incorporated as modules into a number of DGVMs, including LPJ (Sitch et al., 2003), CTEM, CLM3 (Levis et al., 2004), ORCHIDEE (Krinner et al., 2005), SEIB-DGVM (Sato et al., 2007) and CLM4-CND (Oleson et al., 2010).

The major disadvantage of these intermediate complexity fire models is that they are still simplistic concerning certain important aspects of fire, and do not represent all processes related to fire equally well. Glob-FIRM, for example, neglects the availability of ignition sources, the influence of wind speed on fire spread, and aspects such as incomplete combustion of plant material in areas that burned. Fire mortality is set to

GMDD
5, 2347–2443, 2012

a constant PFT-specific rate and does not depend on fire intensity or duration, and annual area burned only depends on the length of the fire season and minimal fuel load. Reg-FIRM leaves trace gas and aerosol emissions from biomass burning unquantified and prescribes vegetation mortality using parameters, similar to Glob-FIRM. CTEM-FIRE does not provide estimates for trace gas and aerosol emissions due to biomass burning. Biomass consumption and plant mortality are prescribed and therefore independent of fire intensity, and the role of litter load and litter moisture is not taken into account explicitly.

Evaluation of intermediate complexity fire modules with remote-sensing based estimates of burned area shows that this class of models has some important deficiencies in simulating realistic patterns of fire globally. Kloster et al. (2010) compared burned area simulated by CTEM-FIRE with the 2001–2009 MODIS Monthly Active Fire Count dataset (Giglio et al., 2006). They conclude that CTEM-FIRE underestimates burned area in certain regions of the world where wildfire is important, including the tropical savannas and the middle-high latitudes over Eurasia. This may be related to the fact that anthropogenic ignition probability and cloud-to-ground lightning ratio are set to globally constant values (0.5 and 0.25, respectively), and to the restrictions in how the burned area in a representative area of 1000 km^2 is calculated.

The most complex representations of fire currently adapted for DGVMs incorporate many of the concepts and equations developed for operational fire forecasting (e.g. Burgan and Rothermel, 1984; Andrews, 1986, 2007; Burgan, 1987; Andrews and Chase, 1989; Reinhardt et al., 1997; Finney, 1998; Andrews et al., 2003, 2008; Heinsch and Andrews, 2010) into a large-scale framework. The first attempts in this direction were already made in the late 1990s, e.g. the MC-FIRE scheme (Lenihan et al., 1998) as part of the MC-DGVM (Bachelet et al., 2003), which allows to explicitly simulate fire spread based on work of Cohen and Deeming (1985) and post fire mortality following Peterson and Ryan (1986), but unrealistically only allows one ignition per grid cell per year. With computational limitations becoming less of an issue, the SPITFIRE (Thonicke et al., 2010) model was developed as a combination of the

GMDD
5, 2347–2443, 2012

intermediate complexity Reg-FIRM and elements of the operational BEHAVE model. SPITFIRE has been incorporated into the LPJ-DGVM (Thonicke et al., 2010), into LPJ-GUESS (Lehsten et al., 2009), and most recently into LPX (Prentice et al., 2011) and used in a variety of applications.

SPITFIRE is run at high temporal resolution for a DGVM (daily time step) and takes into account parameters to distinguish fire behavior among different fuel categories. This complex type of fire model attempts to simulate the complete fire phenomenon based on physical principles. Vegetation dynamics simulated by the DGVM provides the required information about fuel type and fuel load to the fire routine, which in turn will simulate fire occurrence, its impact on the vegetation (partial kill or total kill of plants) and emissions from fire depending on ignition sources and fire weather conditions. Fuel heterogeneity is explicitly accounted for by assigning fuel to different size classes ranging from fine to coarse fuel types, as well as changes in fuel moisture status.

Fire occurrence is determined by ignitions, which can be natural or anthropogenic, as well as by meteorological conditions and availability of fuel. Once the number of ignitions has been determined, the rate of spread depends on fuel characteristics, wind, and topography, although the latter is often not taken into account in fire models for DGVMs. The combination of fuel load, fuel structure and fuel moisture not only affects the rate of fire spread, but directly and indirectly also the intensity and duration of fires and thereby the mortality of plants. The overall consumption of dead and living plant material, combined with the area affected by the fire, determines the emission of CO_2, trace gases (e.g. CH_4, NO_x) and aerosols. Thus, SPITFIRE represents the most comprehensive fire module for DGVMs currently available, and the only one that is potentially able to both represent human-vegetation-fire dynamics and produce quantitative estimates of fire-related trace gas and aerosol emissions for times in the past or future.

At the beginning of the current study, we attempted to use the equations and guidance provided in the model description of SPITFIRE (Thonicke et al., 2010) plus

GMDD
5, 2347–2443, 2012

additional information from the authors (A. Spessa, personal communication, 2011) to implement SPITFIRE into our own version of LPJ with the aim of simulating the dynamics of natural and human-caused fire over the preindustrial Holocene. However, given the information we had, we were not able to reproduce the model results presented in Thonicke et al. (2010).

In the following sections, we describe SPITFIRE-2 LPJ: an improved DGVM that is particularly well-adapted for simulating global fire on centennial to multi-millennial timescales. We outline an evaluation of the new model's based on simulations and observations of fire in Alaska. Simulating fires in Alaska is a good test of the model performance, because it is one of the parts of the world where lightning-caused wildfires in largely intact natural ecosystems dominate the fire regime, and excellent data on historical burned area and lightning ignitions are freely available. It is also a region where fire was systematically underestimated in the original SPITFIRE. Through our presentation of this case study, we highlight the improvements made with the new model. We conclude with recommendations for future developments to this and other global-scale fire models.

2 Rationale for improving SPITFIRE

The original implementation of LPJ-SPITFIRE had several important limitations to its performance. Our implementation of the equations in Thonicke et al. (2010) led to a model that (1) burned too much in some parts of the world and not enough in others, (2) did not represent individual fires that persist for more than one day, (3) oversimplified intra- and inter-annual variability in lightning ignitions, and (4) produced unrealistic estimates of fire rate of spread, particularly in grass fuels. For these reasons, we set out to improve SPITFIRE. Some of the modifications we made to the fire scheme also required modifications to the DGVM itself. A detailed rationale for our improvements is described below.

GMDD
5, 2347–2443, 2012

In the original version of SPITFIRE, tree mortality as a result of fire is unrealistically high in some parts of the world, and results in large parts of the world being dominated by herbaceous vegetation in many places where grasses should not be the main constituents of the landscape. Because herbaceous vegetation has a positive feedback on fire occurrence and spread, increases in simulated grass cover in places where trees had been killed by fire made it impossible for woody vegetation to ever recover.

At the same time, we faced the problems acknowledged in Thonicke et al. (2010) of LPJ-SPITFIRE not being able to simulate fire in boreal regions consistent with observations, e.g. in the MODIS active fire counts product (Giglio et al., 2006) and the GFED3 dataset (Giglio et al., 2010). Moreover, the representation of anthropogenic ignitions remained unclear and unsatisfying, as the authors rely on the usage of the empirical $a(N_D)$ parameter (ignitions individual^{-1} d^{-1}) to describe the propensity of people to produce ignition events. In the best case, $a(N_D)$ could be suitable to describe the relationship between people and fire ignitions at present day, although it is not clear to us how the authors separated anthropogenic from natural wildfire ignitions when they created a global $a(N_D)$ dataset. In any case, this approach of using a prescribed $a(N_D)$ map would have been difficult to apply to describe anthropogenic burning in the past, e.g. over the Holocene, so we needed to develop a different approach to define the relationship between people and fire in preindustrial time.

Further room for improvement was seen in the way fire duration and lightning ignitions are handled in original SPITFIRE. Fires not only influence climate and vegetation, but also feed back on themselves, as fire takes away fuel for consecutive fires and contributes to landscape fractionation, which will counteract large fires. This feedback effect of fire on itself is not represented in the published documentation of the SPITFIRE model, neither is the fact that fires, once started, can burn for multiple days until they run out of fuel, merge with other fires, hit an obstacle or die due to a change in fire weather conditions. Lightning ignitions in SPITFIRE are prescribed from a satellite-based climatology of monthly lightning flash density (Christian, 2003) and smoothly interpolated between months to yield a quasi-daily climatology of lightning strikes (Thonicke et al.,

GMDD
5, 2347–2443, 2012

2010). This approach neither takes into account that lightning tends to occur clustered in time, i.e., it is frequently linked to precipitation events and times of atmospheric instability, nor that lightning can be extremely variable between different years particularly in regions where the total amount of lightning strikes is comparably low. Peterson et al. (2010) describe a linkage between convective available potential energy (CAPE) and cloud-to-ground lightning flashes for Alaska that strongly indicates that specifically at high latitudes where, compared to the low latitudes, the total amount of lightning strikes is low, temporal variability in lightning is substantial and explains for the high variability in observed burned area in boreal ecosystems such as Northern Canada and Alaska. In these regions between 72 % and 93 % of all fires observed at present day are attributed to lightning ignitions (Stocks et al., 2003; Boles and Verbyla, 2000).

Finally, in original SPITFIRE, fire rate of spread is calculated based on weighted averages of variables attributed to the different fuel size classes, e.g. surface-to-volume ratio and packing ratio. We found that this approach of a priori weighting all fuel-related variables according to the mass of the corresponding fuel size class caused a bias in favor of the larger fuel size classes in determining fire rate of spread. We argue that the rate of spread will mostly be determined by the small fuels which are easily ignited due to their high surface-to-volume ratio and low packing density, whereas the role of the larger fuel size classes will be to sustain burning once fire has spread over a given spot. We therefore also propose a different approach for the calculation of the rate of spread, which gives more credit to the role of small, light fuels in fire propagation.

3 Methods

Here we present a new fire module (SPITFIRE-2) that is designed to be used with LPJ and similar DGVMs. The module is based on SPITFIRE (Thonicke et al., 2010), but has been substantially altered in a number of important ways. We made improvements and changes to the calculation of daily lightning ignitions, the fuel bulk density of live fuels, rate of spread and fire mortality. Depending on fire weather conditions, fires are now

GMDD
5, 2347–2443, 2012

allowed to continue burning for multiple days once ignited and are extinguished again either at times when meteorological conditions are not favorable for burning any more, or when fires run out of fuel due to coalescence with other fires or areas that were previously burned and therefore provide no more fuel to propagate further burning. We implemented a simple scheme for crown fires, where, during long-lasting dry conditions when trees experience severe water stress, fire can spread through tree crowns as opposed to on the ground surface. We completely change the way anthropogenic burning is handled by now classifying human populations into three different life subsistence groups (hunter-gatherers, pastoralists, and agriculturalists) based on the assumption that, depending on their lifestyle, people will cause fires for different purposes and to different extents, i.e., different subsistence strategies have different relationships with fire. The new methods of calculating biomass burning required changes not only to SPITFIRE, but also to the LPJ-DGVM, which we also detail in this paper. The model description that follows is presented in the following order:

- Fire ignitions and occurrence (Sect. 3.1)
- Fire spread and dynamics (Sect. 3.2)
- Fire impacts on vegetation (Sect. 3.3)

In each section we detail the representations in SPITFIRE-2 that are different from the original SPITFIRE, followed by any changes we needed to make to LPJ to accommodate the requirements of fire representation. The model description is intended to stand alone, i.e., the entire model can be reconstructed on the basis of the equations and parameters presented in this paper without relying on earlier published descriptions. A comprehensive list of abbreviations is provided in Table 1, a flowchart illustrating the structure of SPITFIRE-2 is depicted in Fig. 1, and a table listing the PFT-specific parameters is presented in Table A1. The remaining equations that were unchanged from original SPITFIRE are detailed in an Appendix, along with a table of supplementary symbols and abbreviations (Table A2).

GMDD
5, 2347–2443, 2012

3.1 Fire ignitions and occurrence

Two major ignition sources for wildfires can be distinguished: natural sources and anthropogenic ignitions. The most common ignition source of naturally developing wildfires is probably lightning ignitions, but other ignition sources such as volcanic eruptions, sparks from rolling rocks or even spontaneous combustion may cause wildfires as well. Humans cause fires either by accident, or purposely for a variety of reasons that will be highlighted in the section on anthropogenic burning.

3.1.1 Factors excluding fire

We only allow fires to start when there is no simulated snow cover in the model, assuming that a snow layer will not allow the spread of surface fires. Also, we do not allow fires if the total vegetation foliar projected cover (FPC) of a given grid cell is less than 50 %, or if the total amount of fuel, including live fuel, all four dead fuel classes and the soil surface carbon pool, is less than $1000\,g\,m^{-2}$, assuming that in these cases a fire might be started, but will not be able to spread far enough from the starting point to cause a significantly large wildfire due to fuels being largely disconnected under such conditions. During model spinup from a bare ground state, we do not allow anthropogenic ignitions of fire before year 800 in order to allow the development of a stable vegetation cover.

3.1.2 Calculation of daily lightning ignitions

For natural burning, lighting strikes are the only source of ignition considered in our fire model. While other natural sources of fire ignitions, such as volcanic eruptions, rolling rocks or spontaneous combustion exist, no global data source is currently available that catalogues the frequency and location of these events. Therefore, natural ignition sources beyond lightning are not taken into account in the fire model. As little global data on the timing and distribution of lightning fire ignitions currently exists, we

GMDD
5, 2347–2443, 2012

needed to develop a relatively involved procedure to estimate daily lightning ignitions. The procedure starts with a climatology of global monthly lightning flashes and disaggregates these into interannually variable daily ground strikes. The actual occurrence of a lightning-caused fire on any given day is a function of the occurrence of ground strikes and the probability of ignition, which is itself a function of fuel type and moisture. A detailed description of the lightning ignitions scheme follows.

To drive our model we used the same lightning dataset that was used in the original SPITFIRE: the LIS/OTD HRMC high-resolution lightning flash climatology (Christian, 2003) (LIS/OTD, http://gcmd.nasa.gov/records/GCMD_lohrmc.html). To our knowledge this is the only currently available climatology of global lightning occurrence, though other datasets, e.g. WWLLN (Virts et al., 2012) and GLD360 (Holle et al., 2011) are under development and could be applied in the future. The LIS/OTD dataset has a 0.5 degree spatial and monthly temporal resolution. We use this dataset as a baseline to provide daily, interannually variable information on lightning occurrence to drive the fire model.

Thonicke et al. (2010) state that they expect the model sensitivity to interannual variability in lightning ignitions to be small compared to the overall model outcome and therefore take this as an argument to neglect interannual variability in lightning. We found that in places where fires are infrequent but important, and generally caused by lightning, e.g. in boreal Alaska and Northern Canada, interannual variability in lightning occurrence is a key component of fire occurrence. We analyzed observations of lightning strikes from the Alaska Lightning Detection System (ALDS, Alaska Bureau of Land Management http://afsmaps.blm.gov/imf/imf.jsp?site=lightning), which revealed that, on a grid cell level, the interannual variability for a given month can be as high as two orders of magnitude. This may well be an explanation for the observed high interannual variability in burned area observed in boreal regions, e.g. in the GFED dataset (Giglio et al., 2010). Peterson et al. (2010) discovered a connection between convective available potential energy (CAPE) and cloud-to-ground lightning flashes for Alaska and Northern Canada, indicating more lightning strikes for times with positive CAPE

GMDD
5, 2347–2443, 2012

anomalies. Using CAPE values from the 20th Century Reanalysis Project (Compo et al., 2011), we determined monthly CAPE anomalies on a grid cell level compared to the 1961–1990 mean CAPE value for a given month, and used these anomalies to create a temporally variable time series of lightning from the LIS/OTD HRMC data set. The largest positive or negative CAPE-anomaly value within the time series for a specific grid cell is used to normalize CAPE anomalies to a range between −1 and 1 for the entire time series available for a given grid cell. Depending on the CAPE-anomaly, the monthly number of lightning flashes is estimated as

$$I_m = \begin{cases} \mathrm{LISOTD}_m \cdot (1 + 9 \cdot \mathrm{CAPE}_{anom}), & \mathrm{CAPE}_{anom} \geq 0 \\ \mathrm{LISOTD}_m \cdot (1 + 0.99 \cdot \mathrm{CAPE}_{anom}), & \mathrm{CAPE}_{anom} < 0 \end{cases} \quad (1)$$

The interannually variable monthly lightning flash data prepared using the procedure described above must be further converted to daily cloud-to-ground lightning strikes to estimate lightning fire ignitions. To accomplish this, we first disaggregated the monthly lightning data to daily estimates using a weather generator based on WGEN (Richardson and Wright, 1984). The monthly number of lighting flashes is disaggregated randomly on all days in the month with precipitation greater than zero. With daily lighting flashes, we estimate ground strikes by using a flash-to-strike ratio of 20 %, as in the original SPITFIRE. We confirmed this flash-to-strike ratio as realistic through a qualitative comparison of lightning ground-strike observations from the ALDS to the satellite-derived flash density in the LIS/OTD HRFC data set.

With an estimate of the daily density of lightning strikes in one gridcell, we then simulate lightning ignitions of wildfire as a function of the efficiency of the fuel in catching fire (ignition efficiency), and a probability that a lightning strike will cause a fire based on Fire Danger Index (FDI) and properties of the landscape. Ignition efficiency reflects the fact that different plant types will more easily catch fire than others as a result of leaf and stem morphology, typical canopy hydration status, and presence of phenols and other flammable compounds in the fuel. In our model, ignition efficiency is specified at the Plant Functional Type (PFT) level, and ranges between 0.05 and 0.5 for

GMDD
5, 2347–2443, 2012

the 9 PFTs used in LPJ ($ieff_{pft}$, Table A1). The average efficiency of a lighting strike to cause a fire is calculated as a weighted average of the PFT-cover and the PFT-specific ignition efficiency of all present PFTs:

$$ieff_{avg} = \frac{\sum_{pft=1}^{npft} (fpc_{grid} \cdot ieff_{pft})}{\sum_{pft=1}^{npft} fpc_{grid}} \quad (2)$$

Lightning strikes do not occur spaced out evenly over landscapes, but will cluster in certain areas, such as mountaintops, tall buildings, etc. Moreover, lightning may strike areas that cannot burn, e.g. rocks, water bodies, or areas that have been burned previously and are therefore deprived of fuel. In order to take this into account, we introduce an additional function to decrease the likelihood of lightning-ignited fires as a function of the area that has already been burned on all previous days of the year:

$$ieff_{bf} = \frac{1 - burnedf}{1 + 25 \cdot burnedf} \quad (3)$$

Finally, the probability that a lightning strike will result in an ignition also depends on the status of the fuel moisture, represented by the fire danger index (FDI). The overall ignition probability on a given day is therefore calculated as:

$$ieff = FDI \cdot ieff_{avg} \cdot ieff_{bf} \quad (4)$$

This probability term, which ranges between 0 and 1, is compared with a uniformly distributed random number between 0 and 1 drawn directly after the calculation of the probability term. If the probability term is greater than the drawn random number, the respective grid cell experiences a lightning-caused ignition on the given day.

GMDD
5, 2347–2443, 2012

3.1.3 Anthropogenic ignitions

Humans have used fire since the Paleolithic as a tool for managing landscapes, for optimizing hunting and gathering opportunities, for cooking, for hunting and defense, and for communication (Pyne, 1994, 1997; Anderson, 1994; Carcaillet et al., 2002; Tinner et al., 2005; Roos et al., 2010). Over the course of history, humans' relationship with fire changed; this was particularly true following the Neolithic revolution when people began cultivating domesticated plants and animals (Iversen, 1941; Kalis and Meurers-Balke, 1998; Lüning, 2000; Rösch et al., 2002; Kalis et al., 2003), and during the 20th century following the institution of industrial fire suppression. As it is our goal to develop a model capable of simulating fire on Holocene timescales, we therefore attempt to distinguish anthropogenic ignitions of fire according to the predominant subsistence strategy of the people living in any given region at any given time. We further account for the physical limits to anthropogenic fire ignitions, the goals of people in igniting fires, and the indirect fire suppression caused by landscape fragmentation.

To simulate anthropogenic fire ignitions, we separate human populations into three groups based on their subsistence lifestyle: hunter-gatherers, pastoralists, and farmers. These three groups cause fire for different purposes and therefore will be distinguishable by their burning behavior. Depending on their lifestyle, people will use fire in a constructive way to manage their habitat (Head, 1994; Bowman, 1998; Bowman et al., 2004). As a result of their mobile lifestyle, hunter-gatherers have the highest motivation to use fire as a tool to manage their habitat in order to promote habitat diversity for game, keep parts of the landscape open in order to be able to move around more easily, and to avoid devastating natural fires by promoting frequent, low intensity fires that remove understory vegetation in forests and reduce fuel loads (Lewis, 1985; Pyne, 1997; Williams, 2000; Kimmerer and Lake, 2001; Stewart et al., 2002). Pastoralists will cause intentional fires to suppress woody encroachment on pastureland and undesired vegetation that animals will not eat, to reduce overgrown fuel loads that can turn small fires into large ones, and to promote new growth of grasses by burning

GMDD
5, 2347–2443, 2012

off old grasses. Crowley and Garnett (2000) list promotion of green-pick, improvement of pasture conditions, creation of fire breaks, control of animal movements, control of stem density, control of weeds and woody encroachment, and control of parasites such as ticks as reasons for pastoralists to use landscape burning as a management tool, while Wincen (1993) also reports usage of fire by pastoralists to improve visibility in mustering. Therefore, their main focus is on the maintenance of good pasture quality, but their burning will be a tradeoff between maintaining good pastures and not burning too much biomass that could be consumed by grazers. Farmers are largely sedentary and therefore will have little interest in burning natural land except for clearance of new cropland and some pasture maintenance for domesticated grazers, but they will burn harvest remainders after crops have been removed from the fields.

One of the major challenges in quantifying anthropogenic burning by any of these groups is to estimate how much fire humans will actually cause. The potential maximum amount of fire that a group of people can cause in a given landscape will depend on the number of people present, their mobility, the vegetation and fuel characteristics of that specific landscape and the prevailing weather conditions. Theoretically, the number of fires that one pre-industrial person can cause on a single day is determined only by how far that person can walk (or ride), assuming that this person can carry a burning torch and can cause un unlimited number of ignitions on the way. What will happen to these ignitions will be determined by the fire weather on that day. If conditions are too wet, none of the ignitions will develop into a fire; if conditions are dry and enough fuel is available most of the ignitions will start off a fire and these fires soon will merge into larger fires, depending on how close the initial ignitions were located from one another and how quickly the fire from these ignitions will spread.

Theoretically, the only limit to how much people can burn will therefore depend on population density, average daily walking range of people, fire weather conditions and fuel availability and structure. In most cases, people will not fully exploit the potential maximum amount of fires they can cause, as they will try to use fire in a constructive way to manage their habitat rather than destroying it by overburning (Head, 1994; Bow-

GMDD
5, 2347–2443, 2012

man, 1998; Bowman et al., 2004). We define this constructive use of fire in terms of burn targets that describe the amount of area burned each group of people will aim to reach on their gridcell in a given year. So instead of prescribing ignition rates or numbers of human ignitions based on $a(N_D)$ values as proposed in Thonicke et al. (2010) we define burn targets for each of the three lifestyle groups that are reached if population density and climatic conditions allow it. Hunter-gatherers will start fires until a maximum of 50 % of the grid cell area has burned within one year, assuming that causing fires beyond this point will become counterproductive for the purposes for which foragers burn. This estimate on hunter-gatherer burning is based on Pyne's (1982) suggestion that Native North Americans repeatedly made controlled surface burns on a cycle of one to three years, broken by occasional catastrophic fires that escaped the area intended to burn and periodic conflagrations during times of drought. Habitat diversity and vegetation patchiness increase with disturbance (in this case fire), but decrease again if disturbance becomes too severe (intermediate disturbance hypothesis, see, e.g. Grime, 1973; Connell, 1978; Huston, 1979; Collins, 1992; Roxburgh et al., 2004; Perry et al., 2011; Faivre et al., 2011). Pastoralists are assigned a burn target of 20 % that they will try to reach before they stop igniting fires, assuming that their interest in causing fires is less pronounced as they will try to preserve biomass for their domesticated grazers, while at the same time trying to maintain good pasture quality and avoid fuel accumulation in fire-prone environments. Being sedentary and concentrating their focus on their crop and pasture land, farmers will mainly burn natural land at the edge of their cultivated land, either to expand cultivated land (slash-and-burn) or to remove fuel and avoid devastating wildfires in the vicinity of where they live. They are assigned an annual burn target of 5 % for burning on natural land.

We allow every 10th person present in a grid cell to ignite fires purposely. This is to take into account that people typically live together in groups and not everybody will need to cause fire, and that some people, such as children or old people, will not be able to walk around and start fires. The average distance that one person lighting fire walks in one day is limited to 10 km. As humans will cause intentional fires mostly at

GMDD
5, 2347–2443, 2012

times when these are beneficial for their purposes, i.e., meteorological conditions allow burning but the overall fire danger is not too high, we restrict anthropogenic burning to days when the average size of single fires, $\bar{a}_f$ will not become larger than 100 ha. In addition, the number of fires started by people on a given day is linked to the FDI via a multiplication factor that reduces the ignitions as FDI increases, with

$$\mathrm{rf} = \begin{cases} 1, & \mathrm{FDI} \leq 0.25 \\ \frac{1}{1.22 \cdot \pi \cdot \mathrm{FDI}} \cdot e^{-\frac{\ln(\mathrm{FDI}+1.29)^2}{0.18}}, & \mathrm{FDI} > 0.25 \end{cases} \quad (5)$$

Intentional fires for land management purposes will therefore preferentially be started when fire danger is low to moderate in order to avoid uncontrolled and unpredictable burning. Anthropogenic ignitions are determined after the calculation of the average size of single fires and their geometry on a given day. The number of individual ignitions per fire-lighting person is calculated as

$$\mathrm{ig_p} = \frac{D_{\mathrm{walk}}}{W_f} \quad (6)$$

where

$$W_f = \frac{\mathrm{DT}}{\mathrm{LB}} \quad (7)$$

The area that one fire-lighting person potentially can burn in one day is given by the equation

$$\mathrm{Ab_{pd}} = \mathrm{ig_p} \cdot \bar{a}_f \quad (8)$$

How much fire people will start on a given day will depend on the environment in which they live. People who live in an environment that naturally has a lot of fire will take into account that some part of the landscape will burn naturally and adjust their

GMDD
5, 2347–2443, 2012

burn target accordingly in order to avoid overburning. Instead they will make smaller burns to prevent the development of large, devastating fires during the most fire-prone time of the year. In order to take into account that people will have a collective memory of the fire history in their habitat, we keep track of the 20-yr running mean of the burned area fraction in a given gridcell, and define the daily burn target for a given livestyle group as

$$\text{target}_{\text{d,group}} = A_{\text{cg}} \cdot \max(\text{target}_{\text{y,group}} - \text{bf}_{20} - \text{burnedf}) \quad (9)$$

In cases where enough fire-lighting people are available to reach or exceed the burn target for the given day, the number of human-caused ignitions is derived from

$$n_{\text{hig}} = \frac{\text{target}_{\text{d,group}}}{\bar{a}_{\text{f}}}, \quad (10)$$

and in cases where the burn target of the day cannot be achieved due to a lack of enough fire-lighting people from

$$n_{\text{hig}} = \text{ig}_{\text{p}} \cdot \text{people}. \quad (11)$$

At present, modern technology allows people for the first time in human history to actively suppress and extinguish wildfires in order to protect their lives and properties. In the past, possibilities to actively suppress and extinguish wildfires were limited (Skinner and Chang, 1996; Pausas and Keeley, 2009). Nevertheless, increases in population densities and parallel increases in land use eventually contributed to landscape fragmentation and thereby indirect suppression of wildfires. This follows the idea of Archibald et al. (2009) that increasing human activities, e.g. grazing, construction of roads, and land cultivation will lead to reduced fuel loads and fuel continuity and increased fragmentation of landscapes, eventually resulting in a reduction of fire spread and therefore spatially less extensive burning.

In order to estimate the effect of increasing land use intensity (fraction of cropland vs. fraction of natural land) we performed a Monte Carlo simulation with a grid of 100 × 100

GMDD
5, 2347–2443, 2012

pixels. We let the fraction of natural land decrease by steps of 0.01 from 1 to zero. For each step, we randomly assigned each pixel within the grid to either be natural land or cropland and calculated the average contiguous area size of natural patches based on an 8-cell neighborhood. To estimate the final average contiguous area size of natural patches, we performed 1000 repetitions of the experiment at each land use fraction. The resulting relation between the natural fraction of a grid cell and the average contiguous area size of natural patches can be approximated by the following equation:

$$\text{ac\_area} = (1.003 + e^{(16.607 - 41.503 \cdot f_{\text{nat}})}) \cdot f_{\text{nat}} \cdot A_{\text{gc}} \quad (12)$$

The average contiguous area size of natural patches is used to set an upper limit to the average size of individual fires ($\bar{a}_{\text{f}}$) in the fire routine. At very high land use fractions, we limit the minimum allowed averaged patch size to a kernel size of 10 ha, not allowing any fragmentation that causes natural patches smaller than this size.

3.1.4 Burning of cropland

Anthropogenic burning of cropland is treated separately from human burning of natural land described above. Burning of croplands can occur independently of weather and fire danger, as managed fields can be burned under almost any weather conditions, e.g. in the uplands of Northwest Europe (Mather, 2004; Dodgshon and Olsson, 2006). Evidence suggests that the usage of fire in cropland management was very common in preindustrial times (see e.g. Dumond, 1961; Sigaut, 1979; Otto and Anderson, 1982; Johnston, 2003; Williams, 2002), and even at present still is in use in parts of the world that rely on subsistence agriculture, e.g. in Sub-Saharan Africa, Southeast Asia, Indonesia and Latin America (Conklin, 1961; Seiler and Crutzen, 1980; Dove, 1985; Smittinand et al., 1986; Unruh et al., 1987; Kleinman et al., 1995; Van Reuler and Janssen, 1996; Cairns and Garrity, 1999; Akanvou et al., 2000; Fox, 2000; Rasul and Thapa, 2003). In SPITFIRE-2, 20 % of the total simulated crop biomass produced within one year remains on the fields as crop remains and is potential fuel for agricultural

GMDD
5, 2347–2443, 2012

burning. Farmers are assumed to burn 20 % of the total cropland area within a grid cell every year. We derived this value from a qualitative comparison between total annual area burned observed in GFED and our simulated burning on natural land for regions in Africa where agricultural burning is still a common practice after harvest. Although this estimate might be too high for some parts of the world and too conservative for others at present day, we believe it is a conservative first approximation for the past when people did not have modern day technology available to prepare fields for the next crop planting after harvest.

3.2 Fire behavior

Once ignited, what happens to fire depends on a number of different environmental factors. Meteorology will directly, e.g. through wind speed, or indirectly, e.g. through temperature, precipitation and duration of dry spells, influence if and how fast ignitions will develop into wildfires, and how large these will eventually grow. Vegetation cover will determine the quality, composition and total amount of available fuel and thereby also influence spread and dynamics of wildfire. The original SPITFIRE model simulated the behavior of surface fires only and allowed fires to burn for only one day. In SPITFIRE-2, we improve upon the original scheme by allowing fires to burn for a number of consecutive days and propose a simple approach to handle multi-day burning and fire dynamics, to model the feedback of fire on itself, and to take the effect of topography on fire spread into account. We also allow fires to spread in tree crowns by introducing a simple scheme to calculate rate of spread in tree crowns depending on the water status of trees. In the following sections we describe the changes and improvements we made to modeling fire behavior since SPITFIRE.

3.2.1 Fuel characteristics

In the process of implementing the new fire routine to LPJ, we noticed larger amounts of fire than expected in certain parts of the world. We traced this back to conditions

GMDD
5, 2347–2443, 2012

of very high fuel loads where large amounts of fuel propagated extremely large fires. This problem was particularly acute in two parts of the world: in the seasonal tropical forests of South America and in the boreal forest. To improve the simulation of fire in both cases, we needed to make several changes to the basic code of LPJ. These changes were very important for simulating realistic amounts and frequency of fires and improve the overall quality of LPJ simulations.

In the seasonal tropics, the total aboveground biomass simulated by LPJ was unrealistically high, leading to unrealistic amounts of litter and thus fuel for fires. In LPJ, too much biomass can be the result of an unrealistically high individual density, or too many large individuals as compared to small individuals. In order to decrease the individual density, we allow trees to grow a larger maximum crown area of 30 m^2 instead of 15 m^2, thus enlarging the maximum possible crown diameter for all tree PFTs from 4.4 m to 6.2 m. At the same time, we increase the maximum sapling establishment rate from 0.12 individual m^{-2} to 0.15 individual m^{-2}. Adjusting these two parameters leads to an overall decrease in total biomass between 5 and 15 %, with highest reduction percentages in areas of high biomass such as the upper Amazon Basin (Fig. 2).

In boreal regions we noticed a different problem, related to unrealistic accumulation of surface fuel. Because litter decomposition is controlled by temperature and moisture in LPJ, simulations in the cold, dry boreal regions of Alaska and Siberia showed very large amounts of aboveground litter, with values as high as 7 kg C m^{-2} in some places. In the fire routine, all fast-decaying litter plus 4.5 % of the total amount of slow aboveground litter is assigned to the fine fuel class (1h-fuel). Given the low bulk density values of the surface fuel prescribed in the original SPITFIRE, these high amounts of surface litter leads to a high accumulation of lightly packed fuel with high surface-to-volume ratios, i.e., a deep fuel bed, and consequently to unrealistically high rates of spread and very large fires. As a consequence, overburning in boreal regions was frequently observed, leading to the permanent establishment of grassland ecosystems where we expected to simulate forests. Although litter breakdown in cold ecosystems may be slow, the assumption that the litter will not be altered mechanically over time

GMDD
5, 2347–2443, 2012

is probably unrealistic. Snow in winter will compact the surface litter from the previous years, the litter structure itself will be altered over time, and a pronounced organic horizon will build up underneath the most recent litter. To take this into account, we defined an additional aboveground soil carbon pool in LPJ that schematically represents an O-horizon. After having calculated decomposition of the three litter pools (fast litter, slow litter and belowground fine litter) as well as the resulting carbon flux from the litter pools to atmosphere and soil pools (cf. Sitch et al., 2003), the remaining carbon in the fast litter pool is transferred to the O-horizon-pool where it decomposes with a turnover time of 2 yr. This way, an organic layer can build up in cold places with slow litter decomposition, but this layer does not affect the rate of spread of surface fires. Carbon that was transferred to the O-horizon does not contribute to the spreading of fires in the rate of spread calculation as it is considered to be packed densely compared to the fuels in the regular fuel size classes, but it is included into the overall fuel combustion term.

We also noticed that fires spread at unrealistically high rates in tundra ecosystems. The original SPITFIRE model assigns a constant fuel bulk density of $2\,\mathrm{kg\,m^{-3}}$ for live grass. We found this to be problematic in tundra ecosystems, where herbaceous and shrubby vegetation grows close to the ground and densely in order to be protected from frost and damage due to the snow burden in winter. Due to the lack of shrub PFTs in LPJ, tundra is represented by the C_3 grass PFT. Using an average live fuel bulk density of $2\,\mathrm{kg\,m^{-3}}$ turns out to cause extensive burning in some northern tundra areas, e.g. in Northern Alaska. In order to take into account the dense growth form of tundra and the general tendency of grassy and herbaceous vegetation to grow denser and closer to the ground with decreasing temperatures, we introduced a dependency between the fuel bulk density of the two grassy PFTs and the 20-yr average number of growing degree days (GDDs):

$$\rho_{\mathrm{livegrass}} = \frac{20\,000}{\mathrm{GDD}_{20} + 1000} - 1 \tag{13}$$

GMDD
5, 2347–2443, 2012

With fewer GDDs, fuel bulk density decreases from typical values in tundra areas around 10–12 $kg\,m^{-3}$, to 1–2 $kg\,m^{-3}$ in warm tropical regions where tall grasses grow.

Finally, we implemented a very simple scheme to represent permafrost conditions. As the moisture content of grass fuels is a function of the top layer soil moisture, unrealistically low soil moisture in boreal and tundra soils where permafrost is present was causing excessive rates of spread and burned area. We estimate the effects of permafrost on soil moisture by impeding the drainage of water out of the soil column. Drainage impedance was implemented for grid cells with a mean annual temperature below 0 °C, in order to simulate permafrost conditions with water being unable to infiltrate into a frozen soil column. As soil frost is not explicitly simulated in LPJ, this represents a simplistic way of simulating permafrost, which will reduce burning in tundra ecosystems by keeping the water status of live fuels high.

3.2.2 Fuel moisture and rate of spread

Differing from the original version of SPITFIRE, we assume that fires will be mostly carried in light fuels as these are easily ignited due to their high surface to volume ratio and low fuel bulk density, whereas heavier fuel components will sustain burning once fire has started at a given place. We therefore calculate rate of fire spread for grassy and woody fuel components separately and then average the two calculated rates of spread according to the coverage of the grassy and woody PFTs on the landscape. To calculate rate of spread in grass, we use a modified form of the equation given in Mell et al. (2012), setting the fuel bulk density for these light fuels equal to the $\rho_{\text{livegrass}}$ value delivered from Eq. (13).

$$\text{ROSf}_{\text{sg}} = \left(0.165 + 0.534 \cdot \frac{U_{\text{f}}}{60}\right) \cdot e^{-0.108 \cdot \text{rm} \cdot 100} \cdot g_{\text{s}} \cdot 60 \tag{14}$$

where

$$g_{\text{s}} = -0.0848 \cdot \min(\rho_{\text{livegrass}}, 12) + 1.0848 \tag{15}$$

GMDD
5, 2347–2443, 2012

to take into account the variable density of live grass depending on GDD20 as calculated in Eq. (13).

For herbaceous fuels, the relative moisture content of the fuel is equal to the ratio

$$\mathrm{rm} = \frac{\omega_{\mathrm{nl}}}{\mathrm{me}_{\mathrm{nl}}} \tag{16}$$

with ω_{nl} being the mean relative moisture content of the 1 h fuel class and the live grass, and $\mathrm{me}_{\mathrm{nl}}$ being the mass-weighted average moisture of extinction for live grass and 1 h fuel. ω_{nl} and $\mathrm{me}_{\mathrm{nl}}$ are calculated as follows:

$$\omega_{\mathrm{nl}} = \frac{\omega(1) \cdot \mathrm{woi}(1) + \omega_{\mathrm{lg}} \cdot (w_{\mathrm{livegrass}} + \mathrm{SOM}_{\mathrm{surf}})}{w_{\mathrm{finefuel}} + \mathrm{SOM}_{\mathrm{surf}}} \tag{17}$$

$$\mathrm{me}_{\mathrm{nl}} = \frac{\mathrm{me}_{\mathrm{fc}}(1) \cdot \mathrm{woi}(1) + \mathrm{me}_{\mathrm{lf}} \cdot (w_{\mathrm{livegrass}} + \mathrm{SOM}_{\mathrm{surf}})}{w_{\mathrm{finefuel}} + \mathrm{SOM}_{\mathrm{surf}}} \tag{18}$$

The rate of spread within the woody fuel components is calculated using the same rate of spread equation as in Thonicke et al. (2010), prescribing a surface area to volume ratio of $5\,\mathrm{cm}^2\,\mathrm{cm}^{-3}$. For details on the calculation of rate of spread, see equations in the appendix to this publication. In the woody case, the relative fuel moisture content is calculated as

$$\mathrm{rm} = \frac{\omega_o}{\mathrm{me}_{\mathrm{avg}}} \tag{19}$$

Instead of setting the relative daily litter moisture back to 100 % as soon as daily precipitation exceeds 3 mm, i.e., Nesterov Index (NI) is set to zero, we calculate ω_o as a mass balance between drying and wetting, assuming that at a threshold of 50 mm precipitation all fuel will be completely wet, and lesser amounts of rain will partially wet the fuel according to the amount of precipitation. The drying term is estimated as

GMDD
5, 2347–2443, 2012

a function of daily maximum and minimum temperature similar to the way the Nesterov Index is calculated in original SPITFIRE:

$$\mathrm{dry_o} = t_{\max} \cdot (t_{\max} - t_{\min} - 4) \cdot \mathrm{caf} \cdot \omega_{\mathrm{o,d-1}} \tag{20}$$

$$\mathrm{wet} = \begin{cases} 1, & \mathrm{prec} > 50\,\mathrm{mm} \\ \frac{\mathrm{prec}}{50} & \mathrm{prec} \le 50\,\mathrm{mm} \end{cases} \tag{21}$$

The water balance between drying and wetting is calculated as follows:

$$\mathrm{balance} = \omega_{\mathrm{o,d-1}} - \mathrm{dry_o} + \mathrm{wet} \tag{22}$$

The fuel moisture on the current day is defined as

$$\mathrm{wet} = \begin{cases} 1, & \mathrm{balance} > 1 \\ \mathrm{balance}, & 0 \le \mathrm{balance} \le 1 \\ 0, & \mathrm{balance} < 0 \end{cases} \tag{23}$$

The parameter caf equals the combined α over all fuels, calculated as

$$\mathrm{caf} = \frac{\sum_{i=1}^{3} \alpha \cdot \mathrm{woi}}{\mathrm{wn}} \cdot \frac{\mathrm{wo}}{\mathrm{wtot}} + \alpha_{\mathrm{lg}} \cdot \frac{w_{\mathrm{livegrass}}}{\mathrm{wtot}} \tag{24}$$

The mass-weighted average moisture of extinction over all fuels, $\mathrm{me_{avg}}$, is calculated as

$$\mathrm{me_{avg}} = \frac{\sum_{i=1}^{\mathrm{fc}} (\mathrm{woi} \cdot \mathrm{me_{fc}})}{\sum_{i=1}^{\mathrm{fc}} \mathrm{woi}} \cdot \frac{\mathrm{wo}}{\mathrm{wtot}} + \frac{\mathrm{me_{lf}} \cdot w_{\mathrm{livegrass}}}{\mathrm{wtot}} \tag{25}$$

GMDD
5, 2347–2443, 2012

Depending on the grasscover fraction of the grid cell, the FDI is calculated as

$$\mathrm{FDI} = \begin{cases} \max(0,(1-\frac{\omega_{\mathrm{nl}}}{\mathrm{me}_{\mathrm{nl}}})), & \text{grasscover} \geq 0.6 \\ \max(0,(1-\frac{\omega_{\mathrm{o}}}{\mathrm{me}_{\mathrm{avg}}})), & \text{grasscover} < 0.6 \end{cases} \quad (26)$$

The surface forward rate of spread is determined by the weighted average between the rate of spread in the woody and herbaceous fuel components according to the cover fractions of trees and grass on the landscape:

$$\mathrm{ROSf_s} = \frac{\mathrm{ROSf_{sw}} \cdot \mathrm{treecover} + \mathrm{ROSf_{sg}} \cdot \mathrm{grasscover}}{\mathrm{treecover} + \mathrm{grasscover}} \quad (27)$$

3.2.3 Simple crown fire scheme

In cases where the total tree cover within a grid cell is 60 % or higher, we assume that the tree crowns are connected enough to support a potential crown fire with flames spreading directly from one tree crown to neighboring ones. We make the likelihood of crown fire dependent on the water status of the crown, with crown fires becoming possible when the canopy experiences water stress. We define water stress as occurring when the mean daily water scalar value (AET/PET) across the tree PFTs present in the grid cell is less than 1 %. The fuel used to calculate the rate of spread in the crown in this case is the sum over all one hour live fuels of the tree PFTs, which are individually calculated as

$$\mathrm{livefuel_{1hr}} = N_{\mathrm{ind}} \cdot 0.045 \cdot (\mathrm{hm_{ind}} + \mathrm{sm_{ind}}) + \mathrm{lm_{ind}} \quad (28)$$

restricted to a maximum value of 8000 $\mathrm{g\,m^{-2}}$. We set the fuel bulk density for the crown fuels to 0.1 $\mathrm{kg\,m^{-3}}$, and the relative moisture content of the crown to 0.99, as living tissue will have high water content even at the point where trees are starting to experience water stress. As fire will predominantly be carried by the small 1 h fuels within the crown, we assign the crown fuel a surface to volume ratio equal to the surface to

GMDD
5, 2347–2443, 2012

volume ratio of the dead 1 h fuel (66 $cm^2\,cm^{-3}$). The overall rate of spread calculated within a grid cell is determined as the maximum of the rate of spread calculated for crown spread and the rate of spread calculated for ground fires:

$$ROSf = \max(ROSf_s, ROSf_c) \quad (29)$$

In case of crown fires, all trees affected by the fire will be killed and their biomass will be transferred to the corresponding litter pools.

3.2.4 Effect of terrain on average fire size

In some parts of the world, terrain may be an important factor influencing the spread of fires. The more complex the terrain, the more likely it will be that the spread of a fire will be impeded by obstacles. Therefore, areas with high relief energy statistically should have smaller average fire sizes compared to areas that are completely flat. Burning down steep slopes may for example decrease the rate of fire spread, and fuel continuity is broken by watercourses and rocky outcrops, or due to higher fuel moisture content on slopes with shady aspect (Guyette et al., 2002). For SPITFIRE-2 we calculated the median slope in a 0.5° gridcell by aggregating slopes calculated at ~ 2 km scale from the ETOPO1 global digital elevation model (Amante and Eakins, 2009, http://www.ngdc.noaa.gov/mgg/global/global.html). Median slope angle at this scale ranges roughly from 0 to 17.2 degrees from horizontal. We define a slope factor as function of the median slope angle of the grid cell as follows:

$$slf = \begin{cases} 1, & \gamma < 1.7^\circ \\ \frac{1}{\frac{5}{9}\pi \cdot \gamma - 2} & \gamma \geq 1.7^\circ \end{cases} \quad (30)$$

This slope factor is used to reduce the default average size of individual fires calculated in the fire routine, $\bar{a}_f$:

$$\bar{a}_f = \bar{a}_f \cdot slf \quad (31)$$

GMDD
5, 2347–2443, 2012

With the size of individual fires being scaled according to the average slope angle, more fires will be required to burn an equivalently sized total area in more complex terrain as compared to flat terrain.

3.2.5 Multi-day burning and coalescence of fires

One of the main problems with the original SPITFIRE was that individual fires could burn for only one day. In places where fire ignitions are rare but large fires do occur, such as in boreal forests, this resulted in very low amounts of fire simulated by the model. In reality, wildfires usually continue burning as long as the fire weather conditions and the availability of fuel do not restrict the progress of the fire (Desiles et al., 2007). To ameliorate the behavior of the model in simulating large, low frequency, large fires we implemented a scheme where we do not extinguish fires at the end of the day, but allow them to burn for multiple days until they burn out due to merging with other fires or areas that already burned during the current year or are put out because of rain. Furthermore, in the original SPITFIRE the Nesterov Index is reset, and therefore FDI, any time more than 3 mm of rain falls in one day. This limit proved to be problematic in our new multi-day burning scheme because ongoing fires were extinguished too easily. To improve the way in which rain affects fire danger and rate of spread, we sum the precipitation amounts on consecutive days and extinguish burning fires only after the precipitation sum exceeds 10 mm for grid cells that have a grass cover of less than 60 %, and 3 mm for grid cells with more than 60 % grass cover. This was implemented to account for the fact that low amounts of precipitation will impede fire spread, but nonetheless fires can keep smoldering and start spreading again as soon as conditions get more dry after a period with low precipitation amounts.

Therefore, the total number of fires burning on a specific day is defined by the number of fires that were started on previous days and have not been extinguished yet, plus a potential additional ignition on the given day that will add another fire. The longer the fire season lasts, the more of the grid cell will already be burned and the likelihood of a fire burning into an area that already burned previously will increase. In such a case,

GMDD
5, 2347–2443, 2012

this fire will run out of fuel as all fuel on the previously burned patch has already been consumed. In order to take this into account, we reduce the number of fires burning on a specific day by the product of the grid cell fraction that already burned this year and the total number of fires on this day. The total number of fires on any given day therefore is calculated as follows:

$$fires_d = fires_{d-1} + fires_{new} - (burnedf \cdot fires_{d-1} + fires_{new}) \quad (32)$$

This implies that with an increased fraction of the grid cell being burned it becomes increasingly more difficult to cause further fires, because they will be more likely to run into an area without fuel or another active fire and be extinguished or merged.

3.3 Fire mortality

Fire mortality in the original version of SPITFIRE was simulated through cambial damage or scorching of tree crowns. In our fire routine, we only allow trees to be killed due to crown scorch and not from cambial damage because the original implementation of cambial kill consistently resulted in too many trees being killed. The time required to critically damage the cambium of trees in the original version of SPITFIRE depends on the thickness of the tree bark, which in turn depends on the stem diameter of the trees. As LPJ treats trees as average individuals, the simulated thickness averaged over different tree ages within a PFT results in trees which are unrealistically small in diameter for their average height and therefore also have unrealistically thin bark, resulting in an overestimation of cambial kill. Furthermore, deciduous trees will only be killed by crown scorch if they have leaves at the time when the fire occurs. This was especially important in parameterizing fire in the seasonal tropics, where frequent fires occur during the dry season but tend not to kill deciduous trees that have very little fuel in, or leading up to, the canopy.

We also re-parameterized the PFT-specific RCK- and p-values which describe the probability of mortality due to crown damage (see Table A1). This recalibration became necessary due to the other modifications in the fire routine in order to avoid

GMDD
5, 2347–2443, 2012

unrealistically high percentages of trees being killed, which in turn would lead to the establishment of permanent grasslands and even more pronounced burning in places where grasslands naturally do not occur.

LPJ requires more than one simulation year to develop a closed grass cover, i.e., the simulation of grass development in LPJ is too slow as grasses usually grow and complete their life cycle within one vegetation period. Due to the unrealistic simulation of grass dynamics within LPJ, removal of grass biomass as a result of burning in one year leads to an underestimation of grass biomass and coverage in the following simulation year. Therefore, we convert the combusted live grass biomass to carbon, but do not remove the grass biomass from the live biomass pool at the end of year in order to mimic a faster development of grasses within the next year and to therefore obtain more realistic biomass and coverage values for grasses when simulating fire. In the future, a new and more realistic implementation for the development and senescence of grasses within LPJ should be implemented.

4 Model results and evaluation

Evaluating a complex DGVM and fire model such as SPITFIRE-2 requires suitable input data sets that can be used to drive the model, including datasets of climate, soils, and lightning strikes, and independent datasets, e.g. satellite data or ground observation data of annual burned area, that can be compared to simulated fire frequency and behavior. Not all parts of the world are equally well represented when it comes to these requirements. In the following sections, we first present and discuss the overall changes to LPJ that we made to improve the simulation of aboveground biomass and O-horizon. We then present our case study for Alaska where we evaluate our model simulation results with reference to the high quality datasets on lightning strikes that we used to drive the model, and detailed maps of annual burned area that we could compare to the model output. Finally we present and discuss a world map of potential

GMDD
5, 2347–2443, 2012

natural fire return interval that could be used for ecosystem management and restoration.

In the simulations described below, we prepared a standard, global driver dataset for LPJ SPITFIRE-2. Climate data to drive the model was derived by applying anomalies derived from the 20th Century Reanalysis project (Compo et al., 2011) to a long term mean climatology based on ClimateWNA and WorldClim 2.1 (Wang et al., 2011; Hijmans et al., 2005, temperature, precipitation, diurnal temperature range), CRU CL 2.0 (New et al., 2002, wind speed, number of wet days), and the Wisconsin HIRS cloud climatology (Wylie et al., 2005, cloud cover). For lightning we used the LIS/OTD data modulated by monthly CAPE anomalies in the procedure described above. We used ETOPO1 for elevation and slope (Amante and Eakins, 2009) and the Harmonized World Soils Database (FAO/IIASA/ISRIC/ISSCAS/JRC, 2008) for soils data. Because we focus on the overall performance of the model in simulating fire behavior and impacts on ecosystems, and because the development of the demographic history datasets is the subject of a separate publication, we exclude anthropogenic ignitions from the simulations presented here. In all of the simulations, the model was spun up to 1870 and then run in a transient simulation to 2010 (the period of the 20th century reanalysis).

4.1 Global biomass

Simulating realistic amounts of biomass for the world's ecosystems is important for modeling reliable amounts of biomass burning and trace gas emissions from wildfires, as the amount of fuel available for burning depends on ecosystem productivity and live biomass. Estimates for biomass in ecosystems of different climatic zones vary largely. Values range between 27 $kg C m^{-2}$ for tropical rainforest and 0.1 $kg C m^{-2}$ for deserts at the high and low end (Blume et al., 2002, Table 3.1–8). Tropical seasonal forests have typical values of 21 $kg C m^{-2}$, followed by deciduous temperate forests with 14 $kg C m^{-2}$, boreal needleleaf forest with 9 $kg C m^{-2}$, savanna with 1.8 $kg C m^{-2}$, steppe with 1.4 $kg m^{-2}$, semi-deserts with 0.35 $kg C m^{-2}$ and tundra ecosystems with biomass

GMDD
5, 2347–2443, 2012

estimates of 0.25 kg C m^{-2}. These values are average estimates and vary significantly depending on site conditions, e.g. soil quality and local climate.

As highlighted in Sect. 3.2.1, living aboveground biomass simulated by LPJ was consistently overestimated compared to values reported in literature, especially in places with high biomass such as the Amazon Basin where simulated values reached a maximum of more than 30 kg C m^{-2}. After the modifications to maximum crown radius and maximum establishment rate simulated aboveground biomass in the Central Amazon Basin now ranges mostly between 18 and 21 kg C m^{-2} (Fig. 2a). In comparison to our simulations (Fig. 2b) shows the C-content of aboveground biomass derived from Saatchi et al. (2009) biomass values using a factor of 0.45 to convert biomass to carbon. For the central part of the Amazon Basin our simulated values are still higher than the satellite-derived estimates of Saatchi et al. (2009), indicating that even after the modifications LPJ's estimates of aboveground live biomass are likely to be still on the high end of estimates. Aboveground biomass carbon estimates collected by Malhi et al. (2006) for old-growth Amazonian forests range between 8.5 and 16.7 kg C m^{-2} assuming a 10.1 % correction term for small trees and lianas in the understory. Estimates of biomass carbon for tropical moist forests in the Brazilian Amazon collected by Houghton et al. (2001) range between 10 and 23.2 kg C m^{-2}, with a mean of 17.7 and a standard deviation of 1.7 kg C m^{-2}. In regions with generally lower biomass, e.g. the Caatinga area or in the Andes, simulated and satellite-derived biomass values reported by Saatchi et al. (2009) are generally in good agreement, though the model underestimates biomass in parts of the Andes.

4.2 The organic soil layer

In their 2004 paper, Pregitzer and Euskirchen (2004) point out that the average amount of carbon stored in organic soil layers, i.e. O-horizons, is highly variable across biomes, and also depends on the age of forest stands, with carbon storage increasing with forest age. Ping et al. (2008) found carbon storage in organic soil horizons to be highly

GMDD
5, 2347–2443, 2012

variable depending on the landscape unit under investigation in the framework of their studies in the arctic tundra of North America, with carbon storage being highest in lowland areas and lowest in mountain areas. Mäkipää (1995) found carbon storage in O-horizons not only to be related to nitrogen availability, but also report C-contents to be highest for mesic sites for their study in Southern Finland.

As described in Sect. 3.2.1, we defined an additional aboveground soil carbon pool in LPJ with the function of an O-horizon to prevent built-up of excessively high amounts of fine fuel litter especially in places with slow litter decomposition by transferring carbon from the fast litter pool to the O-horizon-pool where it decomposes with a turnover time of 2 yr. Although the forest floor can be an important fuel source in forest fires and therefore is included into the combustion process, it has already been structurally and chemically modified by decomposing organisms and the effect of snow cover, therefore making it more compact than the typical fuels that propagate a wildfire. Given the high variability in carbon amounts stored in organic soil layers pointed out above, our approach to incorporate an organic soil layer pool into LPJ is simple, but on a large spatial scale proves to be a good crude approximation (Fig. 3) that helps especially to simulate the spread of fires in boreal forests in an appropriate way. Simulated carbon storage in the organic layer pool is highest in Northeastern Siberia as well as the high latitudes of North America, with values ranging between 2000 and 3500 $g C m^{-2}$. In Scandinavia, simulated values range between 1000 and 2000 $g C m^{-2}$. These values do not capture the high end of values reported in literature, but are well within the observed range. For example, Mäkipää (1995) found C-storage values in organic layers of forest soils in Southern Finland between approx. 500 and 3000 $g C m^{-2}$, depending on nutrient status and site wetness. For the arctic tundra of North America, Ping et al. (2008) reported values between 700 $g C m^{-2}$ for mountain sites on the low end of the observed range, and 15 100 $g C m^{-2}$ for lowland sites on the high end. Pregitzer and Euskirchen (2004) summarize organic soil horizon stocks from a number of studies, giving a range between 200 and 19 500 $g C m^{-2}$ for boreal forests. The values

GMDD
5, 2347–2443, 2012

simulated by LPJ are therefore within a realistic range, although site-specific variability cannot be reproduced on a half-degree resolution grid.

4.3 Fire in boreal ecosystems: the Alaska case study

We found Alaska specifically suitable for our model evaluation, first because the original SPITFIRE was not able to simulate adequate amounts and realistic variability of fire in boreal forests, and second because the availability of datasets to drive and evaluate the fire model is excellent for this region. Fire is an important process in the boreal region and controls a variety of different ecosystem processes such as succession, tree recruitment, vegetation recovery, carbon storage, soil respiration and emission of atmospheric trace gases (Landhaeuser and Wein, 1993; Kurz and Apps, 1999; Johnson, 1992; Harden et al., 2000; Turetsky et al., 2002; Bergner et al., 2004; Kasischke et al., 2005). With their version of LPJ-SPITFIRE, Thonicke et al. (2010) faced the problem of specifically not being able to simulate adequate amounts of fire in boreal regions compared to observational records, e.g. the MODIS active fire counts product (Giglio et al., 2006) or the GFED3 dataset (Giglio et al., 2010). Figure 3 in Thonicke et al. (2010) shows that LPJ-SPITFIRE simulates almost no fire at latitudes northward of 55° N. Due to the highly episodic nature of fires in boreal regions such as Alaska and Northern Canada (Kasischke et al., 2002) most of the burned areas recorded in observational data burned during a limited number of large fire years.

Lightning is the main source of ignitions for large fires in boreal ecosystems. For the period 1950–1969, Barney (1971) showed that ~24 % of all fire ignitions in Alaska were caused by lightning, but fires started by this source accounted for more than 80 % of total area burned. Between 1990 and 1996, on average 31 ± 12 % of all wildfires were caused by lightning, but the average area burned by lightning-caused fires was 89 ± 11 % (Boles and Verbyla, 2000). One of the reasons why the highly variable fluctuations in burned area could not be reproduced by the original version of SPITFIRE could be because interannual variability in lightning occurrence was neglected as described above. Low interannual variability in lightning occurrence may be true for low

GMDD
5, 2347–2443, 2012

latitudes where the total amount of lightning per year is large compared to the variability between different years, but most certainly is not correct for the boreal where the total amount of lightning strikes is generally low and the interannual variability for a given month can be as high as two orders of magnitude. Furthermore, smoldering fires are an important part of boreal and Arctic fire behavior. The recent Anaktuvuk River tundra fire smoldered for nearly two months as the tundra dried out before spreading rapidly at the end of the season (Jones et al., 2009). With the high-quality datasets that were available on fire in Alaska, we set out to see if the improvements we made to LPJ-SPITFIRE substantially improved the model performance in this ecologically important region.

4.3.1 Model setup and datasets

To drive the model specifically for the Alaska case study, we replaced the LIS/OTD global lightning climatology with the ALDS historical lightning ground strike observation data set (described above) for the time period between 1986 and 2011. For the period before 1986, we used the modulated LIS/OTD described in the beginning of Sect. 3.1.2. All other climate and soils data are the same as those described above. Because the majority of land burned in Alaska is due to lightning-ignited fires and most large fires occur in places remote from human settlements where they are not extinguished by humans, we set the model up to only simulate ignition and spread of naturally, i.e., lightning-ignited, fires on land not subject to human land use. To evaluate model performance, we compare simulated area burned between 1986 and 2010 to the historical burned area polygon dataset produced by the Alaska Fire Service (http://afsmaps.blm.gov/imf_firehistory/imf.jsp?site=firehistory). For our comparison, we distinguish the following seven major ecoregions as depicted in Fig. 4:

1. Intermontane Boreal (IB)
2. Arctic Tundra (AT)

GMDD
5, 2347–2443, 2012

3. Arctic Range Transition (ART)
4. Bering Taiga (BTA)
5. Bering Tundra (BTU)
6. Coastal Rainforests (CR)
7. Aleutian Meadows (AM)

4.3.2 Simulated and observed area burned

Depending on the ecoregion in consideration, the simulated and observed area burned in average over the time period from 1986 to 2010 varies considerably. In the following sections, we compare and discuss simulated fire occurrence with observed burned area by ecoregion.

Intermontane Boreal ecoregion

The intermontane boreal ecoregion, situated between the Alaska Range and the Brooks Range, is the most important region of Alaska for fire. On average, 93 % of the total area burned in Alaska is located in this area. Both the observational data and the simulation results identify ecoregion 1 (Intermontane Boreal) as the region most affected by fire. In this region, observations show annual burned area of $4834 \pm 6285\,km^2$ or 0.96 ± 1.25 % of the total area of the region (Table 2). Our simulated annual burned area of $4736 \pm 5654\,km^2$, or 0.94 ± 1.13 %, agrees well with observations, slightly underestimating both the total amount and the magnitude of the interannual variability in burned area. The absolute range of area burned in this region is approximately the same for both the observations and simulation, with a minimum of 136 vs. 0 km^2 and a maximum of 26 464 vs. 25 500 km^2, respectively (Fig. 5). For both observations and simulation, the annual mean burned area is larger than the median, indicating that years with relatively smaller total area burned are frequent, but are interrupted by few

GMDD
5, 2347–2443, 2012

years with very large amounts of annual area burned. In contrast to the mean, where simulated burned area is slightly less than observations, the median and 75 % percentile burned area are slightly greater in the simulation than the observations (Fig. 5).

As shown in Fig. 6, we are able to reproduce the fire behavior observed in the Intermontane Boreal region of Alaska rather well not only in terms of the average area burned over the 25 yr period, but also in terms of the interannual variability.

Arctic Tundra

Compared to the Intermontane Boreal ecoregion described above, burned area in the other six ecoregions is very small in terms of total area burned as well as percent of ecoregion burned (Fig. 5, Table 2). Our simulations therefore correctly identify the location of the most important ecoregion for fire in Alaska. However, our simulations overestimate the mean annual area burned as well as the maximum annual area burned for ecoregion AT (Arctic Tundra) compared to the observation data. This is due to two years within the simulated time series, 2008 and 2009, for which we largely overestimate the total area burned, whereas in most other years we simulate low amounts of burning that match the observational data in magnitude and variability.

The largest fire known to have occurred in the Alaskan Tundra during recent time is the Anaktuvuk River Fire in 2007 that burned an area of approx. 1120 km^2 according to the records of the Alaska Fire Service. This fire was ignited by a lightning strike in mid-July and persisted for almost three months into the first half of October. Close to the Anaktuvuk Fire, a second fire was ignited on the same day less than 10 km to the east. While the Anaktuvuk Fire became the largest fire known in history on the Northern Slope of Alaska, the neighboring Kuparuk Fire only burned approx. 7 km^2 although vegetation and fire weather conditions for both fires were very similar. Where most tundra fires are extinguished by wet soils and dense vegetation, the Anaktuvuk River Fire persisted due to an exceptionally dry summer and smoldered until the tundra was largely dried out and strong southwesterly winds increased the fire rate of spread in September. Most of the total area eventually burned was consumed within less than

GMDD
5, 2347–2443, 2012

one week (Jones et al., 2009). The second-largest fire of the record since 1995, known as fire DCKN190, occurred in 1993, was ignited by lightning and burned 335 km^2 of tundra within approx. one month. Although so far large tundra fires are rather exceptional it is possible that, with potentially warmer summers in the future, fires such as the Anaktuvuk River Fire might become more common in Alaska's northern tundra ecosystems (Jones et al., 2009; Hu et al., 2010).

Bering Taiga and Bering Tundra

Burning in the westernmost part of Alaska (ecoregions BTA and BTU) is generally low in the observation data (Fig. 5, Table 2), with a maximum of 675 km^2 burned during the period from 1986–2010, with an average of 86 $km^2 yr^{-1}$, and a median of 27 $km^2 yr^{-1}$ for the Bering Taiga, and a maximum of 367 $km^2 yr^{-1}$, an average of 48 $km^2 yr^{-1}$ and a median of 0 $km^2 yr^{-1}$ for the Bering Tundra. This implies that in average 0.03 % of the Bering Taiga and 0.05 % of the Bering Tundra region burned over the 25-yr-period. Our simulations underestimate burning in these regions, especially for the Bering Taiga, where the simulated maximum burning is 329 $km^2 yr^{-1}$, with an average of 22 $km^2 yr^{-1}$ and a median of 0 $km^2 yr^{-1}$. For the Bering Tundra, we simulate a maximum of 148 $km^2 yr^{-1}$, an average of 15 $km^2 yr^{-1}$, and a median of 0 $km^2 yr^{-1}$, therefore also underestimating observations.

Ecoregions ART, CR and AM

For ecoregion ART (Alaska Range Transition) we simulate a mean annual burned area of 134 ± 393 $km^2 yr^{-1}$ and a median of 4 $km^2 yr^{-1}$ compared to an observed mean annual burned area of 91 ± 109 $km^2 yr^{-1}$ and a median of 37 $km^2 yr^{-1}$ (Fig. 5, Table 2). We therefore underestimate the median while overestimating the mean, with the latter again being augmented due to one single fire year, 2007, for which we simulate a maximum of 1907 $km^2 yr^{-1}$ against an observation value of only 299 $km^2 yr^{-1}$. All other 24 yr for ecoregion ART are within the range of observation concerning total area burned and

GMDD
5, 2347–2443, 2012

interannual variability. Ecoregions CR (Coastal Rainforest) and AM (Aleutian Meadows) are ecoregions with extremely little amounts of fire observed and simulated, in total as well as percentage of region area. For ecoregion CR, an average of $13 \pm 38\,km^2\,yr^{-1}$ in the observation data compares to a simulated average of $10 \pm 47\,km^2\,yr^{-1}$. Four out of 25 yr with fire have been recorded for ecoregion AM, compared to 2 yr that had fire in the simulation time series. These results reveal that though we may not be able to reproduce exact numbers for area burned at the very low end of fire observations, we are still able to simulate fire occurrence behavior realistically even in areas where burning is rare and getting any fire at all in the simulations is challenging.

4.3.3 Discussion of Alaska burned area results

Figure 6 reveals that peak fire years in our simulated time series do not necessarily match observed peak fire years, which is partially linked to the uncertainty in daily weather conditions resulting from the usage of a weather generator. For example, monthly-resolved climatology constrains precipitation amounts and number of wet days, but the timing of rainy days within a given month may be very different in the simulation compared to the true weather situation, e.g. if simulated wet days all come clustered at the beginning or end of the month whereas in reality they had been more equally distributed over the month. In such a case, the consequences for fuel wetting and drying are different between observation and simulation, with simulation overestimating fuel dryness and FDI and therefore leading to higher amounts of area burned. Moreover, the exact timing of precipitation days also matters for simulating fire extinction, as either one day with more than 10 mm precipitation (3 mm precipitation with more than 60 % grass cover) or several consecutive days with a sum of more than 10 mm precipitation are required to extinguish fires in our simulation. If, for example, a fire is burning in a given month and the simulated clustering of rainy days within this month is less pronounced than the clustering that occurred in reality, the fire may continue burning although in reality it was extinguished. This may also be true for the opposite case, where fires are extinguished although they should have kept burning.

GMDD
5, 2347–2443, 2012

Another uncertainty is linked to wind speed: as we lack a weather generator for disaggregating windspeed to daily estimates, we use climatological mean wind speed, which may underestimate the infrequent, high-wind events that are responsible for the largest episodes of fire spread. Furthermore, we do not simulate the feedback mechanism between fire and wind, e.g. large, intense fires may produce strong convection that increases wind speeds in the vicinity of the fire, which in turn enhances fire spread.

Apart from the uncertainty concerning daily and sub-daily fire weather, we are also not able to simulate the spread of fires from one grid cell into neighboring grid cells, which may lead to un underestimation of burned area in cases where fires start in one $0.5^{\circ} \times 0.5^{\circ}$ grid cell and then burn into adjacent grid cells, a situation that we observed especially for some of the larger fires in the Alaska Fire Service database. With our model setup, we cannot reproduce such fires accurately without needing additional ignitions in these neighboring grid cells, which is a shortcoming of our model.

Correct simulation of fires in tundra regions is challenging for a number of reasons. As our version of LPJ has no specific PFT to represent tundra vegetation, tundra vegetation in the model is covered by the C_3-grass PFT. As described in Sect. 3.2.1, we try to improve the representation of tundra vegetation with respect to fuel conditions by scaling the density of live grasses to the number of growing degree days and by accounting for permafrost-impeded drainage of soil water. Eventually, woody shrub vegetation and tussocks could be represented by one or more separate tundra PFTs (e.g. Kaplan et al., 2003) as each of the constituent tundra vegetation plants have different density, height, and flammability that would affect fire spread. The most significant problem leading to a general overestimation of simulated burned area on the North Slope is the simple soil water scheme of LPJ that is neither able to explicitly simulate permafrost nor wetlands. Detailed analyses of grid pixels in Northern Alaska revealed that soils dry out very quickly as soon as all snow has melted in May or beginning of June, and along with the soil also the live grass moisture drops down quickly as the fire scheme assumes the live fuel moisture to be equal to the moisture of the top soil layer. Summers in Northern Alaska are dry, while at the same time day length is long

GMDD
5, 2347–2443, 2012

and therefore simulated evapotranspiration is high and helps to draw down soil moisture in combination with surface runoff and drainage. Overall, this leads to simulation of environmental conditions that are far drier than in reality where thawing of the active layer proceeds slowly down the soil column over the course of the summer and, by limiting evapotranspiration, keeps soils and vegetation wetter than would otherwise be the case. If lightning occurs in the period between May and July, simulated fires spread very fast and therefore lead to an overestimation of burned area. In most of the cases where we overestimate burning, fires are ignited early in summer when in reality conditions are likely still too wet; the simulated fires spread quickly due to the fuel being dry and keep burning through summer due to the lack of precipitation. In addition to the poor representation of wetlands and permafrost in LPJ, the tundra on Alaska North Slope is characterized by a high density of water bodies, from lakes to streams and rivers on different size scales, which is not taken into account in LPJ. In reality, these water bodies will limit the spread of fires, as can be observed for the Anaktuvuk fire which is bordered by rivers on its western and eastern edge. Future improvements to LPJ and the fire model therefore should focus on the implementation of adequate permafrost and wetland simulation modules (Wania et al., 2009; Koven et al., 2009; Ringeval et al., 2010) and the incorporation of water body density on a grid cell level as limiting factor to the spread of fires.

Comparing the Bering Taiga and Bering Tundra ecoregion to the Arctic Tundra in Northern Alaska reveals that all three ecoregions are characterized by generally very low amounts of lightning. They can therefore be classified as ignition-limited fire regimes. Differing from the Arctic Tundra region, the two western regions have their precipitation maximum in summer, which coincides with the potential fire season. As a consequence of frequent rainfall events with often substantial daily precipitation amounts, fuels often stay rather wet and soil water status is high (Fig. 7). In the already rare case of a lightning ignition, fires therefore tend to spread slowly, stay small and are soon extinguished, especially when compared to fires started in the Arctic Tundra. Given the need to simulate the monthly distribution of wet days and daily precipitation amounts

GMDD
5, 2347–2443, 2012

with a weather generator based on monthly-resolved climatology it is likely to miss the specific circumstances that in reality led to a fire, i.e., hitting the chance of having an ignition while at the same time simulating a sufficiently long dry period after the ignition so that the fire can spread. With only few lightning sensors and weather stations being located in the far west of Alaska, it is also possible that the actual amount of lighting occurring in these two ecoregions is underestimated and not all lighting has been recorded, while at the same time the uncertainty related to the small number of weather stations may bias conditions to be in general more wet than they truly are.

Apart from the limitations discussed here, using daily and interannually variable lightning as described in Sect. 3.1.2 allows us to simulate fire in boreal regions, with results showing considerable interannual variation in total area burned. Although we may not be able to reproduce observed annual area burned exactly on a year-to-year basis due to the points given above, we capture the overall behavior of boreal fires well with SPITFIRE-2 in terms of being able to simulate long-term averages and variability that are consistent with observations.

4.3.4 Simulated fire return intervals in Alaska

Analysis of fire return interval (FRI) is useful for characterizing natural fire regimes and assessing the changes to fire regimes in the past caused by climate change. For the recent past, efforts to reconstruct fire return intervals based on fire scar datasets have been performed by Balshi et al. (2007), who present maps of fire return intervals in boreal North America and Eurasia using historical fire records between 1950–2002/1959–2002 for Alaska/Canada, and ordinary cokriging to interpolate Eurasian FRIs. This enabled the authors to produce interpolated FRI maps for most of the boreal forest (Balshi et al., 2007, Fig. 2). In places where fire is infrequent, however, FRIs may exceed the period of modern observations. Historical records of fire in the boreal forest in the best case hold a little more than 50 yr of data (Alaska, Canada) or even less than that (Eurasia). Short records may be not representative of the overall average fire regime as by chance they may, e.g., represent a time of relatively high or low

GMDD
5, 2347–2443, 2012

fire activity and therefore lead to an overestimation or underestimation of average FRIs over longer time scales. The need to perform spatial interpolation of FRIs over large spatial scales introduces further uncertainty.

While analysis of charcoal accumulation rates from sedimentary archives (lakes, bogs) has been applied successfully on local to regional scales to reconstruct FRIs over longer time scales (e.g. Higuera et al., 2009; Lynch et al., 2004b; Tinner et al., 2006; Higuera et al., 2008; Brubaker et al., 2009), centennial to millennial scale climate variability probably affected FRIs, and it is therefore difficult to characterize the present-day fire regime, or estimate how future climate changes could affect burning, based solely on paleo-archives. The advantage of fire models such as SPITFIRE-2 is that it can be run for long time periods using de-trended steady-state climate, allowing vegetation and fire regime to equilibrate so that conclusions can be made as to what FRIs would be if climate at any given time stayed constant.

To estimate FRIs for Alaska, we made a model run over 1000 yr with steady-state climate after vegetation and fire regime had equilibrated. Following Balshi et al. (2007), we define FRI as the time required to burn an area equal to the entire 0.5° grid cell. The FRI within a grid cell consequently is calculated as the ratio of 1000 yr and the number of times a grid cell area managed to burn during these 1000 yr. We present our simulated fire return intervals in Fig. 8, using the same color scheme as in Balshi et al. (2007), but without applying any smoothing. Agreeing with Balshi et al. (2007), we simulate frequent burning with return intervals between 12 and 50 yr in Eastern Alaska located in the Intermontane Boreal ecoregion between Brooks Range and Alaska Range. Towards the west of ecoregion IB, the FRIs predicted from our simulation become more heterogeneous, mostly ranging between 25 and 50 yr on the high end, and between 400 and 700 yr on the low end, therefore being slightly lower than the FRIs estimated by Balshi et al. (2007). Towards the extreme west of mainland Alaska, we simulate FRIs between 900 and 2000 yr for some grid cells, but mostly FRIs are longer than 2000 yr. Compared to Balshi et al. (2007) we estimate significantly longer FRIs in some grid-cells, especially for ecoregion BTU (Bering Tundra). This may be linked to the potential

GMDD
5, 2347–2443, 2012

wet bias in our climate data mentioned above and the possibility that the already low amounts of lightning are underestimated in the LIS/OTD lightning climatology used for this experiment, due to very short length of record of the lightning climatology and the low detection efficiency at high latitudes. In contrast, we simulate shorter fire return intervals for the Arctic Tundra, which typically fall in the 100–200 yr and 500–700 yr categories. Given the model shortcomings related to the simulation of tundra vegetation and permafrost (see Sect. 4.3.3), these results may be biased somewhat towards the short end.

Our simulated FRIs based on detrended 20th century climatology are a snapshot of a vegetation-fire system in equilibrium with steady-state climate. Reconstructed FRIs based on charcoal records from various sites over Alaska show that fire regimes were subject to changes over the course of the Late Glacial and Holocene (e.g. Lynch et al., 2004b; Tinner et al., 2006; Higuera et al., 2008, 2009; Brubaker et al., 2009) as vegetation and climate changed. Given a scenario of past climate change, our model provides the possibility to simulate changes in fire regime at individual or regionally aggregated charcoal sites and test hypotheses about the drivers of change in fire frequency by comparing simulated FRIs to reconstructed FRIs.

4.4 Global fire under natural conditions

The global effects of fire on aboveground live biomass are demonstrated in Fig. 9. Both panels represent a world with potential natural vegetation and no anthropogenic land use. In panel (a) biomass with natural fires caused by lightning ignitions is shown, panel (b) shows a world without fire. Panel (c) shows the difference in biomass between a world with and without fire. The maps clearly reveal the parts of the world that are mostly affected by fire disturbance and therefore have less biomass than they potentially could have in a world without fire. On a 100 yr basis the total amount of global carbon stored in aboveground live biomass is 208 ± 2 Pg less for the simulation with fire compared to the simulation without fire, totaling 948 ± 3 Pg C with fire. No impact of fire on biomass is simulated for wet tropics, such as the Amazon and Congo Basins or

GMDD
5, 2347–2443, 2012

in Indonesia, all places that naturally store large amounts of carbon in biomass. Most of the biomass loss related to fire disturbance is simulated in the seasonal tropics and subtropics: in the Miombo woodland region south of the Congo Basin, in the east and southeast of the Amazon Basin, in the Sahel, in India and Southeast Asia, and in Northern and Southern Australia. The impact of fire on biomass is also clearly visible in the grassland regions of central and western North America, the Western Mediterranean, Southwestern Russia, Kazakhstan and Uzbekistan. Fires in the boreal regions can be extensive, but the return interval is too long to have a secular impact on carbon storage in aboveground live biomass compared to ecosystems with short fire return intervals.

Global fire return intervals are shown in Fig. 10. As can be seen in the map, fires are most frequent in places where three factors are coincident:

1. enough biomass to sustain frequent burning
2. sufficient amounts of lightning ignitions
3. seasonal meteorological conditions that allow fuel drying

If any of these three conditions is not present, wildfires are unlikely to occur at high frequency. As noted above, fire is rare in the Amazon and Congo Basins and on the Indonesian archipelago. In these regions, lightning ignitions and biomass could support burning, but meteorological conditions are too wet for the development of wildfires. In the desert and high-mountain regions of the world, e.g. the Sahara desert, the southern part of the Arabian Peninsula, and on the Tibetan Plateau, the absence of biomass is the limiting factor for fire. Large parts of the world's boreal and subarctic regions have enough biomass to support frequent burning, but the number of lightning ignitions generally tends to be low compared to lower latitudes, and the presence of snow and temperatures below 0 °C for half a year or more or wet summers limit the frequency of wildfires.

In contrast, in any part of the world where all three factors are met, fire return intervals are short, e.g. in the Sahel, the Western Mediterranean, the Near East, in the Miombo

GMDD
5, 2347–2443, 2012

woodlands south and east of the Congo Basin, in most of Australia, and in the xerophytic Caatinga shrublands of Northeastern Brazil. In some parts of the world we most likely overestimate burning frequency, e.g. in Central Australia, in parts of the Western United States and in Spain. The main reason we simulate too much fire in the first two regions is because LPJ still simulates too much biomass even after the adjustments to maximum crown area and establishment described in Sect. 3.2.1. Live biomass values simulated for Central Australia and the Southwestern USA range between 500 and 1500 $g C m^{-2}$, in some places up to 2000 $g C m^{-2}$. Saatchi et al. (2010, Fig. 3a), show values for total biomass carbon in Central Australia between 0 and 370 $g C m^{-2}$, which would be below the level for which we allow ignitions (see Sect. 3.1.1). For the desert regions of the Southwestern USA, estimates for carbon stored in potential natural vegetation range between 0 and 600 $g C m^{-2}$ (Ruesch and Gibbs, 2008; West et al., 2010). Scheffer-Schachtschabel (Blume et al., 2002, Table 3.1–8, p. 67) report typical biomass C-values of 100 (desert) to 350 (semi-desert) $g m^{-2}$. This indicates that LPJ still overestimates biomass, especially for dry environments, which should be improved in the future by further adapting the drought sensitivities of the PFTs and by introducing a xerophytic shrub type PFT.

In Southern Spain and Northern Morocco, FRI may be overestimated as well, due to the fact that the simulated start of the fire season is very early, often already starting in March or April and then continuing into summer when climatic conditions become dry. In these Mediterranean climate areas, the dominance of low woody vegetation with very deep roots, not simulated in the model, may result in wetter conditions in reality than what we simulate and therefore less likelihood for ignitions in the springtime.

5 General discussion

Realistic simulation of global vegetation dynamics requires the inclusion of disturbance regimes that influence vegetation development, alter vegetation structure and composition and affect global carbon budgets. Simulation of fire, arguably the most important

GMDD
5, 2347–2443, 2012

disturbance process that affects the terrestrial biosphere, is of crucial importance for a more complete model representation of terrestrial vegetation dynamics. Based on the process-based fire model SPITFIRE (Thonicke et al., 2010), we developed a new fire model (SPITFIRE-2) with major improvements to the simulation of fire occurrence, fire spread and fire impact. Under a natural fire regime excluding human interference, lightning is the most common ignition source for wildfires. The timing of lightning ignitions on a daily timescale is important, especially in regions where the total amount of monthly lightning ignitions is low and therefore an equal distribution of lightning strikes on all days within a month may result in significantly underestimating lightning ignitions, e.g. in boreal regions. By correlating the occurrence of lightning strikes with the occurrence of precipitation and using a weather generator and random number generator to do so, we provide a more realistic way to simulate lightning ignitions. The time series of area burned for Central Alaska (Fig. 6) demonstrates that with daily and interannually variable lighting strikes, simulation of realistic fire behavior is possible even in boreal environments where the original SPITFIRE did not simulate any fire.

By allowing the ignition of smoldering fires during wet conditions and simulating fires that persist over the course of multiple days instead of extinguishing each fire at the end of the day when it was ignited, we designed an implementation of fire behavior that better reflects the true behavior of fire. Likewise, the calculation of fuel wetness as a mass balance function of drying and wetting rather than relying on a yes/no decision depending on an arbitrarily chosen precipitation threshold of 3 mm as originally proposed by Thonicke et al. (2010) makes SPITFIRE-2 more successful at realistically simulating fire behavior. We introduced a simple scheme to account for the possible occurrence of crown fires. This basic scheme can serve as basis for future development and incorporation of more sophisticated crown fire schemes, e.g. based on the work of Van Wagner (1977); Rothermel (1991); Cruz et al. (2003); Tachajapong et al. (2008) or Dickinson et al. (2009). Changes in the fuel weighing between grass and woody fuels compared to the original fire scheme put a stronger emphasis on the idea that fire spread will predominantly be influenced by the availability of easily ignitable

GMDD
5, 2347–2443, 2012

smaller fuels, while at the same time, by linking live grass fuel density to climate we account for the different possible growth forms of herbaceous vegetation depending on climatic conditions. Eventually, the introduction of additional shrub PFTs as intermediates between herbaceous vegetation and tree PFTs should be considered, especially for an appropriate representation of tundra and xerophytic shrub vegetation. Introduction of shrub PFTs will help ameliorate the current tendency of the model to overestimate herbaceous vegetation cover in fire prone areas and the strong positive feedback between fire and vegetation that results in an overestimate of fire frequency and the prevalence of grasses, a problem sometimes still observed, for example, in the Arctic tundra of Northern Alaska, or in Southern Spain. Further improvements should also focus on the inclusion of a scheme to simulate wetlands and permafrost in order to capture the way in which permafrost keeps tundra organic matter wet, even under dry meteorological conditions. Because our version of LPJ does not represent permafrost dynamics, soil and fuel drying, and consequently also fire occurrence, are overestimated in wetlands and permafrost areas such as the tundra of the Alaska North Slope.

By introducing a slope factor related to the median slope angle of each 0.5° grid cell, we present a simple way to account for the role that topographic complexity plays in limiting fire size and rate of spread. Eventually, a representation of other natural fire breaks such as rivers and lakes, should be built into the fire module. An approximation of the number of rivers that could act as fire breaks could be handled by using drainage density information extracted from a DEM, but it would also be important to know whether streams were likely to have water in them, as opposed to being dry riverbeds. That rivers constrain the spread of fires can be observed, for example, in case of the large Anaktuvuk River Fire from 2007 in the Alaskan tundra that ultimately was constrained by the two rivers: Nanushuk to the west and Itkillik to the east. Currently, such a measure of fragmentation by water bodies was not at our disposal yet, but is indirectly accounted for using Eq. (32) which links the numbers of fires burning to the area that has been burned before, i.e., the more area has already been burned

GMDD
5, 2347–2443, 2012

the more fires get extinguished and the harder it becomes to burn yet more area within a grid cell.

Because the standard version of LPJ represents vegetation in terms of an "average individual", the model does not simulate the realistic demographic development of forests over time, and the allometry of the resulting individual is unrealistic: e.g., the model tends to simulate very tall trees with thin stems of small diameter and thin bark. This causes problems when simulating the effect of fire on tree mortality, as cambial kill is related to bark thickness and mean residence time of the fire. Therefore, simulating cambial kill using standard empirical relationships based on field observations (Peterson and Ryan, 1986) results in unrealistically high tree mortality, eventually leading to grassland ecosystems in many regions of the world where we expect (fire adapted) forests. In order to simulate cambial kill it would be necessary to have a more realistic demography and allometry for the trees by qualifying the stand-age-structure of woody vegetation, e.g. by simulating explicit cohorts of age classes similar to LPJ-GUESS (Smith et al., 2001) or ED (Moorcroft et al., 2001), or height classes such as TreeMIG (Lischke et al., 2006). Such an approach to vegetation demography also would allow accounting for the fact that ground fires will affect trees differently according to their size and age, with effects being most severe for recruitment of young trees, whereas fire-adapted larger individuals may survive ground fires. The drawback of using an explicit scheme for vegetation dynamics is that the computational demand is increased by 1–2 orders of magnitude, thus making multi-millennial model integrations more difficult. Finally, grass PFTs should be implemented such that they are able to reach full cover and complete their lifecycle within one year's growing season. To accomplish this it would be necessary to run the entire model, including vegetation dynamics, at a daily timestep, but this will again increase computational demand by roughly an order of magnitude.

Humans are known to have used fire as a tool for landscape management since at least the middle Palaeolithic (Mason, 2000; Bowman et al., 2009; Ritter, 2011; Haws, 2012; Berna et al., 2012). Fire regimes throughout the Holocene are arguably more

GMDD
5, 2347–2443, 2012

influenced by human activities than by natural processes, particularly in subtropical and temperate ecosystems (Pyne, 1997; Bowman et al., 2009, 2011). The original SPITFIRE was designed for present-day conditions where fire suppression is the primary control on the fire regime in many parts of the world. As we intend to use the fire model for simulations of palaeofire regimes on Holocene timescales, we needed to develop a completely new implementation of anthropogenic burning. Literature research, evidence from palaeoproxies such as charcoal, and discussions with anthropologists and archaeologists led us to the conclusion that humans in the past used fire for a variety of different reasons, depending on their lifestyles and their living environment, and that terrestrial biomass burning related to human activity must have been very common. By developing a method of representing the way in which people with different subsistence lifestyles interact with fire, with SPITFIRE-2 we are now able to perform quantitative estimates on the impact of anthropogenic burning on vegetation, carbon pools and trace gas emissions on a global scale during preindustrial time.

6 Conclusions

Beginning with an implementation of SPITFIRE from Thonicke et al. (2010), we made improvements to several aspects of the original formulation, achieved a more realistic process representation of fire occurrence, fire behavior, and fire impacts, and solved many of the deficiencies of the original model. With our new fire module, SPITFIRE-2, we were able to simulate realistic fire regimes in Alaska, one of the key regions of the boreal forest where SPITFIRE results were unsatisfactory. We also developed a scheme to distinguish among the ways in which pre-industrial people with different subsistence strategies interact with fire to achieve their land management goals. The updated fire model SPITFIRE-2 is a major improvement on past global fire models and will be particularly useful for studying changes in global fire on millennial timescales. We hope that SPITFIRE-2 will be useful for us and others to perform process-based

GMDD
5, 2347–2443, 2012

simulations of terrestrial biomass burning, while at the same time providing a solid basis for further improvements, modifications and model development.

Appendix A

In this appendix we provide the equations used in SPITFIRE-2 that were not changed from the original SPITFIRE. With these, we provide a complete documentation of SPITFIRE-2. Variable and parameter abbreviations used in addition to those in Table 1 are provided in Table A2.

A1 Fuel load and moisture

Fuel calculation by PFT and by fuel type ("slow aboveground litter" includes all woody litter, whereas "fast aboveground litter" is leaves only):

$$\mathrm{df(PFT,1)} = 2.22 \cdot (s(1) \cdot \mathrm{las(PFT)} + \mathrm{laf(PFT)}) \quad \text{(A1)}$$

$$\mathrm{df(PFT,2:4)} = 2.22 \cdot (s(2:4) \cdot \mathrm{las(PFT)}) \quad \text{(A2)}$$

$$\mathrm{lf(PFT,1)} = 2.22 \cdot N_{\mathrm{ind}} \cdot (s(1) \cdot (\mathrm{hm_{ind}(PFT)} + \mathrm{sm_{ind}(PFT)}) + \mathrm{lm_{ind}(PFT)}) \quad \text{(A3)}$$

$$\mathrm{lf(PFT,2:4)} = 2.22 \cdot N_{\mathrm{ind}} \cdot s(2:4) \cdot (\mathrm{hm_{ind}(PFT)} + \mathrm{sm_{ind}(PFT)}) \quad \text{(A4)}$$

s = 0.045, 0.075, 0.21, 0.67 for fuel size classes 1–4. Dead fuel load per fuel size class:

$$\mathrm{woi(class)} = \sum_{\mathrm{pft}=1}^{\mathrm{npft}} \mathrm{df(pft,class)} \quad \text{(A5)}$$

Relative moisture content of live grass fuel:

$$\omega_{\mathrm{lg}} = \frac{10}{9} \cdot \omega_{\mathrm{s1}} - \frac{1}{9} \quad \text{(A6)}$$

GMDD
5, 2347–2443, 2012

Recalculation of α_{lg}:

$$\alpha_{lg} = \begin{cases} \frac{-\log \omega_{lg}}{NI}, & \omega_{lg} > 0 \quad \text{and} \quad NI > 0 \\ 0, & \text{else} \end{cases} \tag{A7}$$

Calculation of total fine fuel amount:

$$w_{finefuel} = \text{woi}(1) + w_{livegrass} \tag{A8}$$

Total mass of dead fuel summed across the first three fuel classes and all PFTs:

$$\text{wo} = \sum_{class=1}^{3} (\text{woi}(class)) \tag{A9}$$

Total dead fuel mass within the first three fuel size classes, plus mass of the live grass:

$$\text{wtot} = \text{wo} + w_{livegrass} \tag{A10}$$

GMDD
5, 2347–2443, 2012

A2 Rate of spread

For the calculation of $ROSf_{sw}$, $\sigma = 5$,

$$rel_m = \frac{\omega_o}{me_{avg}} \tag{A11}$$

$$wn = livemass + deadmass \tag{A12}$$

$$livemass = \sum_{PFT=8}^{9} pftlivefuel(PFT) \tag{A13}$$

$$deadmass = \sum_{PFT=1}^{9} pftdeadfuel(PFT) \tag{A14}$$

$$pftlivefuel(PFT) = \sum_{class=1}^{3} lf(PFT,class) \tag{A15}$$

$$pftdeadfuel(PFT) = \sum_{class=1}^{3} df(PFT,class) \tag{A16}$$

$$\rho_{PFT(PFT)} = \frac{\rho_{b,PFT(PFT)} \cdot Z}{\sum_{class=1}^{3} df(PFT,class)} \tag{A17}$$

$$Z = df(PFT,1) + 1.2 \cdot df(PFT,2) + 1.4 \cdot df(PFT,3) \tag{A18}$$

$$\rho_b = \frac{\rho_{livegrass} \cdot livemass + \sum_{i=1}^{npft} (\rho_{PFT(i)} \cdot pftdeadfuel(i))}{wn} \tag{A19}$$

GMDD
5, 2347–2443, 2012

For the calculation of $ROSf_c$, $\sigma = 66$, $rel_m = 0.99$, $\rho_b = 0.1$, and

$$wn = \min\left(\sum_{PFT=1}^{7} lf(PFT,1), 8000\right) \quad \text{(A20)}$$

The actual rate of spread calculation is based on Eqs. (A21) to (A38).

Packing ratio:

$$\beta = \frac{\rho_b}{\rho_p} \quad \text{(A21)}$$

Optimum packing ratio:

$$\beta_{op} = 0.200395 \cdot \sigma^{-0.8189} \quad \text{(A22)}$$

Ratio of packing ratio to optimum packing ratio:

$$p_{ratio} = \frac{\beta}{\beta_{op}} \quad \text{(A23)}$$

Maximum reaction velocity:

$$\Gamma'_{max} = \frac{1}{0.0591 + 2.926 \cdot \sigma^{-1.5}} \quad \text{(A24)}$$

Optimum reaction velocity:

$$\Gamma' = \Gamma'_{max} \cdot p_{ratio}^{A} \cdot e^{A \cdot (1 - p_{ratio})} \quad \text{(A25)}$$

$$A = 8.9033 \cdot \sigma^{-0.7913} \quad \text{(A26)}$$

Moisture dampening coefficient:

$$v_M = 1 - 2.59 \cdot rel_m + 5.11 \cdot rel_m^2 - 3.52 \cdot rel_m^3 \quad \text{(A27)}$$

GMDD
5, 2347–2443, 2012

Reaction intensity:

$$IR = \Gamma' \cdot wn \cdot h \cdot \nu_M \cdot \nu_s \tag{A28}$$

Ratio of propagating flux to reaction intensity:

$$\xi = \frac{e^{(0.792+3.7597\cdot\sqrt{\sigma}\cdot(\beta+0.1))}}{192+7.9095\cdot\sigma} \tag{A29}$$

Wind coefficient:

$$\Phi_w = C \cdot (3.281 \cdot U_{forward})^B \cdot p_{ratio}^{-E} \tag{A30}$$

$$C = 7.47 \cdot e^{-0.8711\cdot\sigma^0.55} \tag{A31}$$

$$B = 0.15988 \cdot \sigma^{0.54} \tag{A32}$$

$$E = 0.715 \cdot e^{-0.01094\cdot\sigma} \tag{A33}$$

Effective heating number:

$$\epsilon = e^{\frac{-4.528}{\sigma}} \tag{A34}$$

Heat of pre-ignition:

$$Q_{ig} = 581 + 2594 \cdot \omega_o \tag{A35}$$

Wind multiplier for high-wind conditions: at a wind speed of $10\,m\,s^{-1}$ and above, the calculated ROS will be doubled, as the BEHAVE-based ROS is increasingly too low at higher wind speeds (see Fig. 13, Morvan et al., 2008):

$$windfact = \begin{cases} 1 + e^{2\cdot U_{forward}} - 20, & \frac{U_{forward}}{60} \leq 10 \\ 2, & \frac{U_{forward}}{60} > 10 \end{cases} \tag{A36}$$

GMDD
5, 2347–2443, 2012

The rate of spread is then calculated as follows:

$$\mathrm{ROS_x} = \frac{\mathrm{IR} \cdot \xi \cdot (1 + \Phi_\mathrm{w}) \cdot \mathrm{windfact}}{\rho_\mathrm{b} \cdot \epsilon \cdot Q_\mathrm{ig}} \quad \text{(A37)}$$

Backward rate of spread (decreases with increasing wind speed):

$$\mathrm{ROSb_s} = \mathrm{ROSf_s} \cdot e^{-0.012 \cdot U_\mathrm{forward}} \quad \text{(A38)}$$

A3 Fire geometry and duration

Length-to-breadth ratio of burn ellipse in cases when wind speeds exceeds 1 km h^{-1}:

$$\mathrm{LB_{tree}} = 1 + 8.729 \cdot (1 - e^{-0.03 \cdot 0.06 \cdot U_\mathrm{forward}})^{2.155} \quad \text{(A39)}$$

$$\mathrm{LB_{grass}} = 1.1 + 0.06 \cdot {U_\mathrm{forward}}^{0.0464} \quad \text{(A40)}$$

$$\mathrm{LB} = \min(\mathrm{LB_{tree}} \cdot \mathrm{treecover} + \mathrm{LB_{grass}} \cdot \mathrm{grasscover}, 8) \quad \text{(A41)}$$

In cases when wind speed is slower than 1 km h^{-1}, LB = 1. The maximum daily fire duration is derived as a function of FDI:

$$t_\mathrm{fire} = \frac{241}{1 + 240 \cdot e^{-11.06 \cdot \mathrm{FDI}}} \quad \text{(A42)}$$

The total distance traveled by a fire within a day is estimated as

$$\mathrm{DT} = t_\mathrm{fire} \cdot (\mathrm{ROSf} + \mathrm{ROSb}) \quad \text{(A43)}$$

The mean area burned by one single fire is calculated as

$$\bar{a}_\mathrm{f} = \min\left(\frac{\pi}{4 \cdot \mathrm{LB}} \cdot \mathrm{DT}^2 \cdot 0.0001 \cdot \mathrm{slf}, \mathrm{ac\_area}\right) \quad \text{(A44)}$$

GMDD
5, 2347–2443, 2012

A4 Combustion of dead fuel

Fraction of live grass consumed by surface fire:

$$\mathrm{rm} = \frac{\omega_{\mathrm{lg}}}{\mathrm{me}_{\mathrm{lf}}} \tag{A45}$$

$$\mathrm{CF}_{\mathrm{lg}} = \begin{cases} 1, & \mathrm{rm} \le 0.18 \\ 2.45 - 2.45 \cdot \mathrm{rm}, & \mathrm{rm} > 0.73 \\ 1.10 - 0.62 \cdot \mathrm{rm}, & \text{else} \end{cases} \tag{A46}$$

Fraction of 1 h fuel consumed by surface fire:

$$\mathrm{rm} = \frac{\omega(1)}{\mathrm{me}_{\mathrm{fc}}(1)} \tag{A47}$$

$$\mathrm{CF}(1) = \begin{cases} 1, & \mathrm{rm} \le 0.18 \\ 2.45 - 2.45 \cdot \mathrm{rm}, & \mathrm{rm} > 0.73 \\ 1.10 - 0.62 \cdot \mathrm{rm}, & \text{else} \end{cases} \tag{A48}$$

Fraction of 10-h fuel consumed by surface fire:

$$\mathrm{rm} = \frac{\omega(2)}{\mathrm{me}_{\mathrm{fc}}(2)} \tag{A49}$$

$$\mathrm{CF}(2) = \begin{cases} 1, & \mathrm{rm} \le 0.12 \\ 1.47 - 1.47 \cdot \mathrm{rm}, & \mathrm{rm} > 0.51 \\ 1.09 - 0.72 \cdot \mathrm{rm}, & \text{else} \end{cases} \tag{A50}$$

GMDD
5, 2347–2443, 2012

Fraction of 100-h fuel consumed by surface fire:

$$\mathrm{rm} = \frac{\omega(3)}{\mathrm{me_{fc}}(3)} \tag{A51}$$

$$\mathrm{CF}(3) = \begin{cases} 0.98 - 0.85 \cdot \mathrm{rm}, & \mathrm{rm} \le 0.38 \\ 1.06 - 1.06 \cdot \mathrm{rm}, & \text{else} \end{cases} \tag{A52}$$

Fraction of 1000-h fuel consumed by surface fire:

$$\mathrm{rm} = \frac{\omega(4)}{\mathrm{me_{fc}}(4)} \tag{A53}$$

$$\mathrm{CF}(4) = -0.8 \cdot \mathrm{rm} + 0.8 \tag{A54}$$

Total fuel consumed in each fuel size class:

$$\mathrm{FC(class)} = \mathrm{CF(class)} \cdot \mathrm{woi(class)} \cdot (1 - \mathrm{ST}) \tag{A55}$$

Calculation of surface fire intensity:

$$I_{\mathrm{surface}} = h \cdot \mathrm{ROSf_s} \cdot \sum_{\mathrm{class}=1}^{3} \mathrm{FC(class)} \cdot \frac{1}{60} \tag{A56}$$

If the surface fire intensity is less than $50\,\mathrm{kW\,m^{-1}}$, it is considered to be too low for burning and fires are extinguished.

A5 Fire mortality and combustion of live fuel

Due to the problems described above related to the average individual concept of LPJ, we only allow trees to be killed due to crown scorch. For seasonally leaf-bearing trees, crown scorch is relevant as long as there are leaves on the tree.

GMDD
5, 2347–2443, 2012

Probability of mortality due to crown damage, calculated per PFT:

$$P_{\mathrm{mCK}}(\mathrm{PFT}) = \mathrm{RCK}(\mathrm{PFT}) \cdot \mathrm{CK}(\mathrm{PFT})^3 \cdot \mathrm{dphen}(\mathrm{PFT}) \quad \text{(A57)}$$

$$\mathrm{CK}(\mathrm{PFT}) = \frac{\mathrm{SH}(\mathrm{PFT}) - \mathrm{height}(\mathrm{PFT}) + \mathrm{CL}(\mathrm{PFT})}{\mathrm{CL}(\mathrm{PFT})} \quad \text{(A58)}$$

$$\mathrm{SH}(\mathrm{PFT}) = F(\mathrm{PFT}) \cdot I_{\mathrm{surface}}{}^{0.667} \quad \text{(A59)}$$

$$\mathrm{CL}(\mathrm{PFT}) = \max(\mathrm{height}(\mathrm{PFT}) \cdot \mathrm{CLf}(\mathrm{PFT}), 0.01) \quad \text{(A60)}$$

A6 Fuel consumption

Biomass burned from dead fuel by fuel type and PFT:

$$\mathrm{BB}_{\mathrm{dead(PFT,1)}} = \mathrm{AB}_{\mathrm{frac}} \cdot \mathrm{CF}(1) \cdot \mathrm{laf}(\mathrm{PFT}) \quad \text{(A61)}$$

$$\mathrm{BB}_{\mathrm{dead(PFT,2)}} = \mathrm{AB}_{\mathrm{frac}} \cdot \mathrm{CF}(1) \cdot \mathrm{las}(\mathrm{PFT}) \cdot 0.045 \quad \text{(A62)}$$

$$\mathrm{BB}_{\mathrm{dead(PFT,3)}} = \mathrm{AB}_{\mathrm{frac}} \cdot \mathrm{CF}(2) \cdot \mathrm{las}(\mathrm{PFT}) \cdot 0.075 \quad \text{(A63)}$$

$$\mathrm{BB}_{\mathrm{dead(PFT,4)}} = \mathrm{AB}_{\mathrm{frac}} \cdot \mathrm{CF}(3) \cdot \mathrm{las}(\mathrm{PFT}) \cdot 0.21 \quad \text{(A64)}$$

$$\mathrm{BB}_{\mathrm{dead(PFT,5)}} = \mathrm{AB}_{\mathrm{frac}} \cdot \mathrm{CF}(4) \cdot \mathrm{las}(\mathrm{PFT}) \cdot 0.67 \quad \text{(A65)}$$

These are calculated on a daily basis. To calculate the annual total, the daily sum is accumulated over the course of the year:

$$\mathrm{annBB}_{\mathrm{dead(PFT)}} = \mathrm{annBB}_{\mathrm{dead(PFT)}} + \mathrm{BB}_{\mathrm{dead(PFT)}} \quad \text{(A66)}$$

Biomass burned from live fuel by fuel type and PFT:
For tree-type PFTs:

$$\mathrm{BB}_{\mathrm{live(PFT,1)}} = \mathrm{AB}_{\mathrm{frac}} \cdot \mathrm{CK}(\mathrm{PFT}) \cdot \mathrm{lm}_{\mathrm{ind(PFT)}} \cdot N_{\mathrm{ind(PFT)}} \quad \text{(A67)}$$

$$\mathrm{BB}_{\mathrm{live(PFT,2)}} = \mathrm{AB}_{\mathrm{frac}} \cdot \mathrm{CK}(\mathrm{PFT}) \cdot \mathrm{sm}_{\mathrm{ind(PFT)}} \cdot N_{\mathrm{ind(PFT)}} \cdot 0.04875 \quad \text{(A68)}$$

$$\mathrm{BB}_{\mathrm{live(PFT,3)}} = \mathrm{AB}_{\mathrm{frac}} \cdot \mathrm{CK}(\mathrm{PFT}) \cdot \mathrm{hm}_{\mathrm{ind(PFT)}} \cdot N_{\mathrm{ind(PFT)}} \cdot 0.04875 \quad \text{(A69)}$$

GMDD
5, 2347–2443, 2012

For grass-type PFTs:

$$BB_{live(PFT,1)} = AB_{frac} \cdot CF(1) \cdot lm_{ind(PFT)} \quad (A70)$$

Annual totals are continuously summed over the course of the year:

$$annBB_{live(PFT)} = annBB_{live(PFT)} + BB_{live(PFT)} \quad (A71)$$

The annual running sum of mortality probability is calculated as:

$$ann_{kill(PFT)} = ann_{kill(PFT)} + P_{mCK(PFT)} \cdot AB_{frac} \quad (A72)$$

In case of crownfire, the mortality probability is assumed to be 100 %:

$$ann_{kill(PFT)} = ann_{kill(PFT)} + AB_{frac} \quad (A73)$$

Updating of the litter pools is done once at the end of the year:

$$laf(PFT) = \max(laf(PFT) - annBB_{dead(PFT,1)}, 0) \quad (A74)$$

$$las(PFT) = \max(las(PFT) - \sum_{i=2}^{5} annBB_{dead(PFT,i)}, 0) \quad (A75)$$

For the tree-type PFTs, live biomass that was killed but not consumed by burning is transferred to the litter pools and the individual density is updated based on the fraction of individuals that were killed over the course of the year:

$$N_{ind\text{-}kill(PFT)} = ann_{kill(PFT)} \cdot N_{ind(PFT)} \quad (A76)$$

$$laf(PFT) = laf(PFT) + N_{ind\text{-}kill(PFT)} \cdot lm_{ind(PFT)} \quad (A77)$$

$$las(PFT) = las(PFT) + N_{ind\text{-}kill(PFT)} \cdot (sm_{ind(PFT)} + hm_{ind(PFT)}) \quad (A78)$$

$$lbg(PFT) = lbg(PFT) + N_{ind\text{-}kill(PFT)} \cdot rm_{ind(PFT)} \quad (A79)$$

$$N_{ind(PFT)} = \max(N_{ind(PFT)} - N_{ind\text{-}kill(PFT)}, 0) \quad (A80)$$

In case of a PFT being killed off completely by fire, reset presence to "false" and set all biomass pools of that PFT ($lm_{ind(PFT)}, sm_{ind(PFT)}, hm_{ind(PFT)}, rm_{ind(PFT)}$) to zero.

GMDD
5, 2347–2443, 2012

A7 Trace gas emissions

Total carbon emissions from burning, across all PFTs:

$$BB_{tot} = \sum_{PFT=1}^{npft} \sum_{i=1}^{5} BB_{dead(PFT,i)} + \sum_{PFT=1}^{npft} \sum_{j=1}^{3} BB_{live(PFT,j)} \quad (A81)$$

To calculate annual total carbon flux from biomass burning, keep updating the running sum:

$$acflux_{fire} = acflux_{fire} + BB_{tot} \quad (A82)$$

Amount of carbon emissions from burning, per PFT:

$$BB_{pft(PFT)} = 0.001 \cdot 2.22 \cdot \sum_{i=1}^{5} BB_{dead(PFT,i)} + \sum_{j=1}^{3} BB_{live(PFT,j)} \quad (A83)$$

Daily trace gas emissions per species:

$$Mx(spec) = \sum_{PFT=1}^{npft} (emfact(PFT,spec) \cdot BB_{pft(PFT)}) \quad (A84)$$

Annual trace gas emissions per species are calculated as running sum over the year:

$$aMx(spec) = aMx(spec) + Mx(spec) \quad (A85)$$

Acknowledgements. We would like to thank Allan Spessa for helpful discussions during the implementation process of originial SPITFIRE. Funding for this work was provided by grants from the Swiss National Science Foundation (PP0022-1190049) and the Italian Ministery for Research and Education (FIRB RBID08LNFJ) for the Research Project CASTANEA.

GMDD
5, 2347–2443, 2012

References

Akanvou, R., Becker, M., Chano, M., Johnson, D. E., Gbaka-Tcheche, H., and Toure, A.: Fallow residue management effects on upland rice in three agroecological zones of West Africa, Biol. Fert. Soils, 31, 501–507, 2000. 2368

Amante, C. and Eakins, B. W.: ETOPO1 1 Arc-minute Global Relief Model: procedures, data sources and analysis, NOAA technical memorandum, nesdis ngdc-24, NOAA, 2009. 2376, 2380

Anderson, M. K.: Prehistoric anthropogenic wildland burning by hunter-gatherer societies in the temperate regions: a net source, sink, or neutral to the global carbon budget?, Chemosphere, 29, 913–934, 1994. 2363

Andreae, M. O.: Biomass burning: its history, use, and distribution and its impacts on environmental quality and global climate, in: Global Biomass Burning: Atmospheric, Climatic, and Biospheric Implications, MIT Press, Cambridge, Massachusetts, USA, 3–21, 1991. 2349

Andreae, M. O. and Merlet, P.: Emission of trace gases and aerosols from biomass burning, Global Biogeochem. Cy., 15, 955–966, 2001. 2349

Andrews, P. L.: BEHAVE: fire behavior prediction and fuel modeling system – burn subsystem, Part 1, General Technical Report INT-194, United States Department of Agriculture, Forest Service, Intermountain Research Station, Ogden, UT 84401, 1986. 2351, 2353

Andrews, P. L.: BehavePlus fire modeling system: past, present, and future, in: Proceedings of the 7th Symposium on Fire and Forest Meteorological Society, Bar Harbor, ME, Am. Meteorol. Soc., 23–25 October 2007, 2007. 2351, 2353

Andrews, P. L. and Chase, C. H.: BEHAVE: fire behavior prediction and fuel modeling system – BURN subsystem, Part 2, General Technical Report INT-260, United States Department of Agriculture, Forest Service, Intermountain Research Station, Ogden, UT 84401, 1989. 2351, 2353

Andrews, P. L., Bevins, C. D., and Seli, R. C.: BehavePlus fire modeling system, version 2.0: users guide, General technical report, United States Department of Agriculture, Forest Service, Rocky Mountain Research Station, Ogden, UT, 2003. 2351, 2353

Andrews, P. L., Bevins, C. D., and Seli, R. C.: BehavePlus fire modeling system, version 4.0: users guide, General Technical Report RMRS-GTR-106WWW Revised, United States Department of Agriculture, Forest Service, Rocky Mountain Research Station, Ogden, UT, 2008. 2351, 2353

GMDD
5, 2347–2443, 2012

Anshari, G., Kershaw, A. P., and van der Kaars, S.: A Late Pleistocene and Holocene pollen and charcoal record from peat swamp forest, Lake Sentarum Wildlife Reserve, West Kalimantan, Indonesia, Palaeogeogr. Palaeoclimatol. Palaeoecol., 171, 213–228, 2001. 2349

Archibald, S. A., Roy, D. P., van Wilgen, B. W., and Scholes, R. J.: What limits fire? An examination of drivers of burnt area in Southern Africa, Glob. Change Biol., 15, 613–630, 2009. 2351, 2367

Arora, V. K. and Boer, G. J.: Fire as an interactive component of dynamic vegetation models, J. Geophys. Res., 110, G02008, doi:10.1029/2005JG000042, 2005. 2352

Bachelet, D., Neilson, R. P., Hickler, T., Drapek, R. J., Lenihan, J. M., Sykes, M. T., Smith, B., Sitch, S., and Thonicke, K.: Simulating past and future dynamics of natural ecosystems in the United States, Global Biogeochem. Cy., 17, 1045, doi:10.1029/2001GB001508, 2003. 2353

Balshi, M. S., McGuire, A. D., Zhuang, Q., Melillo, J., Kicklighter, D. W., Kasischke, E., Wirth, C., Flannigan, M., Harden, J., Clein, J. S., Burnside, T. J., McAllister, J., Kurz, W. A., Apps, M., and Shvidenko, A.: The role of historical fire disturbance in the carbon dynamics of the pan-boreal region: a process-based analysis, J. Geophys. Res., 112, G02029, doi:10.1029/2006JG000380, 2007. 2391, 2392

Barney, R. J.: Wildfires in Alaska - some historical and projected effects and aspects, Proceedings – Fire in the Northern Environment – A Symposium, College AK, 13–14 April 1971, 51–59, US Forest Service, Portland, OR, 1971. 2383

Belillas, C. M. and Rodà, F.: The effects of fire on water quality, dissolved nutrient losses and the export of particulate matter from dry heathland catchments, J. Hydrol., 150, 1–17, 1993. 2349

Bergner, B., Johnstone, J., and Treseder, K. K.: Experimental warming and burn severity alter CO_2 flux and soil functional groups in recently burned boreal forest, Glob. Change Biol., 10, 1996–2004, 2004. 2383

Berna, F., Goldberg, P., Horwitz, L. K. H., Brink, J., Holt, S., Bamford, M., and Chazan, M.: Microstratigraphic evidence of in situ fire in the Acheulean strata of Wonderwerk Cave, Northern Cape province, South Africa, Proc. Natl. Acad. Sci., p. 6, doi:10.1073/pnas.1117620109, 2012. 2398

Blume, H.-P., Brümmer, G. W., Schwertmann, U., Horn, R., Kögel-Knabner, I., Stahr, K., Auerswald, K., Beyer, L., Hartmann, A., Litz, N., Scheinost, A., Stanjek, H., Welp, G., and Wilke, B.: Scheffer/Schachtschabel – Lehrbuch der Bodenkunde, 15th edn., Spektrum Akademischer Verlag GmbH, Heidelberg, Berlin, 2002. 2380, 2395

GMDD
5, 2347–2443, 2012

Boles, S. H. and Verbyla, D. L.: Comparison of three AVHRR-based fire detection algorithms for interior Alaska, Remote Sens. Environ., 72, 1–16, 2000. 2357, 2383
Bond, W. J. and van Wilgen, B. W.: Fire and Plants, Chapman & Hall, London, UK, 1996. 2349
Bond, W. J., Woodward, F. I., and Midgley, G. F.: The global distribution of ecosystems in a world without fire, New Phytol., 165, 525–538, doi:10.1111/j.1469-8137.2004.01252.x, 2005. 2349
Bowman, D. M. J. S.: Tansley review No. 101 – The impact of Aboriginal landscape burning on the Australian biota, New Phytol., 140, 385–410, 1998. 2363, 2364
Bowman, D. M. J. S., Walsh, A., and Prior, L. D.: Landscape analysis of Aboriginal fire management in Central Arnhem Land, North Australia, J. Biogeogr., 31, 207–223, 2004. 2363, 2365
Bowman, D. M. J. S., Balch, J. K., Artaxo, P., Bond, W. J., Carlson, J. M., Cochrane, M. A., D'Antonio, C. M., DeFries, R. S., Doyle, J. C., Harrison, S. P., Johnston, F. H., Keeley, J. E., Krawchuck, M. A., Kull, C. A., Marston, J. B., Moritz, M. A., Prentice, I. C., Roos, C. I., Scott, A. C., Swetnam, T. W., van der Werf, G. R., and Pyne, S. J.: Fire in the Earth system, Science, 324, 481–485, 2009. 2349, 2398, 2399
Bowman, D. M. J. S., Balch, J., Artaxo, P., Bond, W. J., Cochrane, M. A., D'Antonio, C. M., DeFries, R., Johnston, F. H., Keeley, J. E., Krawchuck, M. A., Kull, C. A., Mack, M., Moritz, M. A., Pyne, S. J., Roos, C. I., Scott, A. C., Sodhi, N. S., and Swetnam, T. W.: The human dimension of fire regimes on Earth, J. Biogeogr., 38, 12, 2223–2236, doi:10.1111/j.1365-2699.2011.02595.x, 2011. 2399
Boyd, M.: Identification of anthropogenic burning in the palaeoecological record of the Northern Prairies: a new approach, Ann. Assoc. Am. Geogr., 92, 471–487, 2002. 2349
Brubaker, L., Higuera, P. E., Rupp, T. S., Olson, M. A., Anderson, P. M., and Hu, F. S.: Linking sediment-charcoal records and ecological modeling to understand causes of fire-regime change in boreal forests, Ecology, 90, 1788–1801, 2009. 2392, 2393
Burgan, R. E.: Concepts and interpreted examples in advanced fuel modeling, General Technical Report INT-283, United States Department of Agriculture, Forest Service, Intermountain Research Station, Ogden, UT 84401, 1987. 2351, 2353
Burgan, R. E. and Rothermel, R. C.: BEHAVE: fire behavior prediction and fuel modeling system – fuel subsystem, General Technical Report INT-167, National Wildfire Coordinating Group, United States Department of Agriculture, United States Department of the Interior, Intermountain Forest and Range Experiment Station, Ogden, UT 84401, 1984. 2351, 2353

GMDD
5, 2347–2443, 2012

Busch, D. E. and Smith, S. D.: Effects of fire on water and salinity relations of riparian woody taxa, Oecologia, 94, 186–194, 1993. 2349
Bush, M. B., Silman, M. R., de Toledo, M. B., Listopad, C., Gosling, W. D., Williams, C., de Oliveira, P. E., and Krisel, C.: Holocene fire and occupation in Amazonia: records from two lake districts, Philos. T. Roy. Soc. B, 362, 209–218, 2007. 2349
Cairns, M. and Garrity, D. P.: Improving shifting cultivation in Southeast Asia by building on indigenous fallow management strategies, Agroforest. Syst., 47, 37–48, 1999. 2368
Carcaillet, C.: A spatially precise study of holocene fire history, climate and human impact within the Maurienne Valley, North French Alps, British Ecol. Soc., 86, 384–396, 1998. 2349
Carcaillet, C., Almquist, H., Asnong, H., Bradshaw, R. H. W., Carrión, J. S., Gaillard, M.-J., Gajewski, K., Haas, J. N., Haberle, S. G., Hadorn, P., Müller, S. D., Richard, P. J. H., Richoz, I., Rösch, M., Sánchez Goñi, M. F., von Stedingk, H., Stevenson, A. C., Talon, B., Tardy, C., Tinner, W., Tryterud, E., Wick, L., and Willis, K. J.: Holocene biomass burning and global dynamics of the carbon cycle, Chemosphere, 49, 845–863, 2002. 2349, 2363
Cerdà, A. and Doerr, S. H.: Influence of vegetation recovery on soil hydrology and erodibility following fire: an 11-year investigation, Int. J. Wildland Fire, 14, 423–437, 2005. 2349
Christian, H. J.: Global frequency and distribution of lightning as observed from space by the optical transient detector, J. Geophys. Res., 108, 4005, doi:10.1029/2002JD002347, 2003. 2356, 2360
Clark, J. S.: Fire and climate change during the last 750 yr in Northwestern Minnesota, Ecol. Monogr., 60, 135–159, 1990. 2349
Cohen, J. D. and Deeming, J. E.: The National Fire Danger Rating System: basic equations, General Technical Report PSW-GTR-82,23, Pacific Southwest Forest and Range Experiment Station, Berkeley, 1985. 2353
Collins, S. L.: Fire frequency and community heterogeneity in Tallgrass Prairie vegetation, Ecology, 73, 2001–2006, 1992. 2365
Compo, G. P., Whitacker, J. S., Sardeshmukh, P. D., Matsui, N., Allan, R. J., Yin, X., Gleason Jr., B. E., Vose, R. S., Rutledge, G., Bessemoulin, P., Brönnimann, S., Brunet, M., Crouthamel, R. I., Grant, A. N., Groisman, P. Y., Jones, P. D., Kruk, M. C., Kruger, A. C., Marshall, G. J., Maugeri, M., Mok, H. Y., Nordli, Ø., Ross, T. F., Trigo, R. M., Wang, X. L., Woodruff, S. D., and Worley, S. J.: The Twentieth Century Reanalysis Project, Quart. J. Roy. Meteorol. Soc., 137, 1–28, 2011. 2361, 2380
Conklin, H. C.: The study of shifting cultivation, Curr. Anthropol., 2, 27–61, 1961. 2368

GMDD
5, 2347–2443, 2012

SPITFIRE-2: an improved fire module for DGVMs

M. Pfeiffer and J. O. Kaplan

Connell, J. H.: Diversity in tropical rain forests and coral reefs, Science, 199, 1302–1310, 1978. 2365
Cox, P. M.: Description of the TRIFFID Dynamic Global Vegetation Model, Tech. Rep. Tech. Note 24, Hadley Center, Bracknell, UK, 2001. 2352
Crowley, G. M. and Garnett, S. T.: Changing fire management in the pastoral lands of Cape York Peninsula of Northeast Australia, 1623 to 1996, Austr. Geogr. Stud., 38, 10–26, 2000. 2364
Crutzen, P. J. and Andreae, M. O.: Biomass burning in the tropics: impact on atmospheric chemistry and biogeochemical cycles, Science, 250, 1669–1678, 1990. 2349
Cruz, M. G., Alexander, M. E., and Wakimoto, R. H.: Assessing canopy fuel stratum characteristics in crown fire prone fuel types of Western North America, Int. J. Wildland Fire, 12, 39–50, 2003. 2396
Desiles, S. L. E., Nijssen, B., Ekwurzel, B., and Ferré, T. P. A.: Post-wildfire changes in suspended sediment rating curves: Sabino Canyon, Arizona, Hydrol. Process., 21, 1413–1423, 2007. 2377
Dickinson, J. D., Robinson, A. P., Gessler, P. E., Harrod, R. J., and Smith, A. M. S.: Flatland in flames: a two-dimensional crown fire propagation model, Int. J. Wildland Fire, 18, 527–535, 2009. 2396
Dixon, R. K., Brown, S., and Houghton, R. A.: Carbon pools and flux of global forest ecosystems, Science, 263, 185–190, 1994. 2349
Dodgshon, R. A. and Olsson, G. A.: Heather moorland in the Scottish Highlands: the history of a cultural landscape, 1600–1880, J. Hist. Geogr., 32, 21–37, 2006. 2368
Dove, M. R.: Swidden Agriculture in Indonesia: the Subsistence Strategies of the Kalimantan Kantu, Mouton de Gruyter, Berlin, Germany, 1985. 2368
Dumond, D. E.: Swidden agriculture and the rise of the Maya civilization, Southwest. J. Anthropol., 17, 301–316, 1961. 2368
Dwyer, E., Pinnock, S., Grégoire, J.-M., and Pereira, J. M. C.: Global spatial and temporal distribution of vegetation fire as determined from satellite observations, Int. J. Remote Sens., 21, 1289–1302, 2000. 2349
Fahenstock, G. R. . and Agee, J. K.: Biomass consumption and smoke production by prehistoric and modern forest fires in Western Washington, J. Forest., 81, 653–657, 1983. 2349

GMDD
5, 2347–2443, 2012

Faivre, N., P., R., Boer, M. M., McCaw, L., and Grierson, P. F.: Characterization of landscape pyrodiversity in Mediterranean environments: contrasts and similarities between South-Western Australia nd South-Eastern France, Landscape Ecol., 26, 557–571, 2011. 2365
FAO/IIASA/ISRIC/ISSCAS/JRC: Harmonized World Soil Database (version 1.0), FAO, Rome, Italy, IIASA, Laxenburg, Austria, 2008. 2380
Finney, M. A.: FARSITE: Fire Area Simulator – model development and evaluation, USDA Forest Service Research Paper, RMRS-RP-4 Revised, 52, Missoula, MT, 1998. 2351, 2353
Foster, D., Swanson, F., Aber, J., Burke, I., Brokaw, N., Tilman, D., and Knapp, A.: The importance of land-use legacies to ecology and conservation, BioScience, 53, 77–88, 2003. 2349
Fox, J. M.: How blaming "slash and burn" farmers is deforesting mainland Southeast Asia, AsiaPacific Issues, 47, 1–8, 2000. 2368
Gavin, D. G., Brubaker, L. B., and Lertzman, K. P.: Holocene fire history of a coastal temperate rain forest based on soil charcoal radiocarbon dates, Ecology, 84, 186–201, 2003. 2349
Giglio, L., van der Werf, G. R., Randerson, J. T., Collatz, G. J., and Kasibhatla, P.: Global estimation of burned area using MODIS active fire observations, Atmos. Chem. Phys., 6, 957–974, doi:10.5194/acp-6-957-2006, 2006. 2353, 2356, 2383
Giglio, L., Randerson, J. T., van der Werf, G. R., Kasibhatla, P. S., Collatz, G. J., Morton, D. C., and DeFries, R. S.: Assessing variability and long-term trends in burned area by merging multiple satellite fire products, Biogeosciences, 7, 1171–1186, doi:10.5194/bg-7-1171-2010, 2010. 2356, 2360, 2383
Grime, J. P.: Control of species density in herbaceous vegetation, J. Environ. Manage., 1, 151–167, 1973. 2365
Grimm, E. C.: Fire and other factors controlling the big wood vegetation of Minnesota in the mid-nineteenth century, Ecol. Monogr., 54, 291–311, 1984. 2349
Guyette, R. P., Muzika, R. M., and Dey, D. C.: Dynamics of an anthropogenic fire regime, Ecosystems, 5, 472–486, 2002. 2376
Haberle, S. G. and Ledru, M.-P.: Correlations among charcoal records of fires from the past 16,000 years in Indonesia, Papua New Guinea, and Central and South America, Quat. Res., 55, 97–104, 2001. 2349
Harden, J. W., Trumbore, S. E., Stocks, B. J., Hirsch, A., Gower, S. T., O'Neill, K. P., and Kasischke, E. S.: The role of fire in the boreal carbon budget, Glob. Change Biol., 6, 174–184, 2000. 2383

GMDD
5, 2347–2443, 2012

Haws, J. A.: Paleolithic socionatural relationships during MIS3 and 2 in Central Portugal, Quat. Int., 254, 61–77, 2012. 2398
Head, L. M.: Landscapes socialised by fire: post-contact changes in Aboriginal fire use in Northern Australia, and implications for prehistory, Archaeol. Ocean., 29, 172–181, 1994. 2349, 2363, 2364
Heinsch, F. A. and Andrews, P. L.: BehavePlus fire modeling system, version 5.0: design and features, General Technical Report RMRS-GTR-249, United States Department of Agriculture, Forest Service, Rocky Mountain Research Station, Fort Collins, CO, 2010. 2351, 2353
Higuera, P. E., Brubaker, L. B., Anderson, P. M., Brown, T. A., Kennedy, A. T., and Hu, F. S.: Frequent fires in ancient shrub tundra: implications of paleorecords for Arctic environmental change, PLoS One, 3, e0001744, doi:10.1371/journal.pone.0001744, 2008. 2392, 2393
Higuera, P. E., Brubaker, L. B., Anderson, P. M., Hu, F. S., and Brown, T. A.: Vegetation mediated the impacts of postglacial climate change on fire regimes in the South-Central Brooks Range, Alaska, Ecol. Monogr., 79, 2009. 2392, 2393
Hijmans, R. J., Cameron, S. E., Parra, J. L., Jones, P. G., and Jarvis, A.: Very high resolution interpolated climate surfaces for global land areas, Int. J. Climatol., 25, 1965–1978, 2005. 2380
Holle, R. L., Cummins, K. L., and Demetriades, N. W. S.: Monthly distribution of NLDN and GLD360 cloud-to-ground lightning, Tech. rep., Vaisala Inc., Tucson, Arizona 85756, 2011. 2360
Houghton, R. A., Hackler, J. L., and Lawrence, K. T.: Changes in terrestrial carbon storage in the United States, 2: the role of fire and fire management, Global Ecol. Biogeogr., 9, 145–170, 2000. 2349
Houghton, R. A., Lawrence, K. T., Hackler, J. L., and Brown, S.: The spatial distribution of forest biomass in the Brazilian Amazon: a comparison of estimates, Glob. Change Biol., 7, 731–746, 2001. 2381
Hu, F. S., Higuera, P. E., Walsh, J. E., Chapman, W. L., Duffy, P. A., Brubaker, L. B., and Chipman, M. L.: Tundra burning in Alaska: linkages to climatic change and sea ice retreat, J. Geophys. Res., 115, 8, doi:10.1029/2009JG001270, 2010. 2387
Huston, M.: A general hypothesis of species diversity, Am. Nat., 113, 81–101, 1979. 2365
Iversen, J.: Landnam i Danmarks Stenalder, En pollenanalytisk Undersøgelse over det første Landbrugs Indvirkning paa Vegetationsudviklingen, (Land occupation in Denmark's Stone

GMDD
5, 2347–2443, 2012

Age, a pollen-analytical study of the influence of farmer culture on the vegetational development), Danmarks Geologiske Undersølgelse, Raekke II, 1941. 2363

Jain, A. K., Tao, Z., Yang, X., and Gillespie, C.: Estimates of global biomass burning emissions for reactive greenhouse gases (CO_2, NMHCs, and NO_x) and CO_2, J. Geophys. Res., 111, 14 pp., doi:10.1029/2005JD006237, 2006. 2349

Johnson, D. W., Susfalk, R. B., Dahlgren, R. A., and Klopatek, J. M.: Fire is more important than water for nitrogen fluxes in semi-arid forests, Environ. Sci. Policy, 1, 79–86, 1998. 2349

Johnson, E. A.: Fire and Vegetation Dynamics: Studies from the North American Boreal Forest, Cambridge University Press, Cambridge, 1992. 2383

Johnston, K. J.: The intensification of pre-industrial cereal agriculture in the tropics: boserup, cultivation lengthening, and the Classic Maya, Anthropol. Archaeol., 22, 126–161, 2003. 2368

Jones, B. M., Kolden, C. A., Jandtt, R., Abatzoglout, J. T., Urbans, F., and Arp, C. D.: Fire behavior, weather, and burn severity of the 2007 Anaktuvuk River Tundra fire, North Slope, Alaska, Arct. Antarct. Alpine Res., 41, 309–318, doi:10.1657/l938-4246-41.3.309, 2009. 2384, 2387

Kalis, A. J. and Meurers-Balke, J.: Die "Landnam"-Modelle von Iversen und Troels-Smith zur Neolithisierung des westlichen Ostseegebietes – ein Versuch ihrer Aktualisierung, Prähist. Z., 73, 1–24, 1998. 2363

Kalis, A. J., Merkt, J., and Wunderlich, J.: Environmental changes during the Holocene climatic optimum in Central Europe – human impact and natural causes, Quat. Sci. Rev., 22, 33–79, 2003. 2363

Kaplan, J. O., Bigelow, N. H., Prentice, I. C., Harrison, S. P., Bartlein, P. J., Christensen, T. R., Cramer, W., Matveyeva, N. V., McGuire, A. D., Murray, D. F., Razzhivin, V. Y., Smith, B., Walker, D. A., Anderson, P. M., Andreev, A. A., Brubaker, L. B., Edwards, M. E., and Lozhkin, A. V.: Climate change and Arctic ecosystems: 2. modeling, paleodata-model comparisons, and future projections, J. Geophys. Res., 108, 8171, doi:10.1029/2002JD002559, 2003. 2389

Kasischke, E. S., Williams, D., and Barry, D.: Analysis of the patterns of large fires in the boreal forest of Alaska, Int. J. Wildland Fire, 11, 131–144, 2002. 2383

Kasischke, E. S., Hyer, E. J., Novelli, P. C., Bruhwiler, L. P., French, N. H. F., Sukhinin, A. I., Hewson, J. H., and Stocks, B. J.: Influences of boreal fire emissions on Northern Hemisphere atmospheric carbon and carbon monoxide, Global Biogeochem. Cy., 19, GB1012, doi:10.1029/2004GB002300, 2005. 2383

GMDD
5, 2347–2443, 2012

Keeley, J. E., Fotheringham, C. J., and Morais, M.: Reexamining fire suppression impacts on brushland fire regimes, Science, 284, 1829–1832, 1999. 2349
Kimmerer, R. W. and Lake, F. K.: The role of indigenous burning in land management, J. Forest., 99, 36–41, 2001. 2349, 2363
Kleinman, P. J. A., Pimentel, D., and Bryant, R. B.: The ecological sustainability of slash-and-burn agriculture, Agricult. Ecosyst. Environ., 52, 235–249, 1995. 2368
Kloster, S., Mahowald, N. M., Randerson, J. T., Thornton, P. E., Hoffman, F. M., Levis, S., Lawrence, P. J., Feddema, J. J., Oleson, K. W., and Lawrence, D. M.: Fire dynamics during the 20th century simulated by the Community Land Model, Biogeosciences, 7, 1877–1902, doi:10.5194/bg-7-1877-2010, 2010. 2353
Koven, C., Friedlingstein, P., Ciais, P., D., K., Krinner, G., and Tarnocai, C.: On the formation of high-latitude carbon stocks: effects of cryoturbation and insulation by organic matter in a land surface model, Geophys. Res. Lett., 36, 5 pp., L21501, doi:10.1029/2009GL040150, 2009. 2390
Krinner, G., Viovy, N., de Noblet-Ducoudré, N., Ogée, J., Polcher, J., Friedlingstein, P., Ciais, P., Sitch, S., and Prentice, I. C.: A dynamic global vegetation model for studies of the coupled atmosphere-biosphere system, Global Biogeochem. Cy., 19, GB1015, doi:10.1029/2003GB002199, 2005. 2352
Kucharik, C. J., Foley, J. A., Delire, C., Fisher, V. A., coe, M. T., Lenters, J. D., Young-Molling, C., and Ramankutty, N.: Testing the performance of a Dynamic Global Ecosystem Model: water balance, carbon balance, and vegetation structure, Global Biogeochem. Cy., 14, 795–525, 2000. 2352
Kurz, W. A. and Apps, M. J.: A 70-year retrospective analysis of carbon fluxes in the Canadian forest sector, Ecol. Appl., 9, 526–547, 1999. 2383
Landhaeuser, S. M. and Wein, R. M.: Postfire vegetation recovery and tree establishment at the Arctic treeline: climatic-change-vegetation-response hypothesis, J. Ecol., 81, 665–672, 1993. 2383
Lehsten, V., Tansey, K., Balzter, H., Thonicke, K., Spessa, A., Weber, U., Smith, B., and Arneth, A.: Estimating carbon emissions from African wildfires, Biogeosciences, 6, 349–360, doi:10.5194/bg-6-349-2009, 2009. 2354
Lenihan, J. M., Daly, C., Bachelet, D., and Neilson, R. P.: Simulating broad-scale fire severity in a Dynamic Global Vegetation Model, Northwest Sci., 72, 91–103, 1998. 2353

GMDD
5, 2347–2443, 2012

Levis, S., Bonan, G. B., Vertenstein, M., and Oleson, K. W.: The Community Land Model's Dynamic Global Vegetation Model (CLM-DGVM): technical description and user's guide, Tech. Rep. NCAR Tech. Note TN-459-IA, NCAR, Terrestrial Sciences Section, Boulder, Colorado, 2004. 2352

Lischke, H., Zimmermann, N. E., Bolliger, J., Rickebusch, S., and Löffler, T. J.: TreeMig: a forest-landscape model for simulating spatio-temporal patterns from stand to landscape scale, Ecol. Model., 199, 409–420, 2006. 2398

Long, C. J., Whitlock, C., Bartlein, P. J., and Millspaugh, S. H.: A 9000-fire history from the Oregon Coast Range, based on a high-resolution charcoal study, Can. J. Forest Res., 28, 774–787, 1998. 2350

Lewis, H. T.: Why Indians Burned: Specific Versus General Reasons, GTR-INT-182, in: Proceedings – Symposium and Workshop on Wilderness Fire: Missoula, Montana, Ogden, UT: USDA Forest Service, edited by: Lotan, J. E., Kilgore, W. C., Fisher, W. C., and Mutch, R. W., Intermountain Forest and Range Experiment Station, Ogden, UT 84401, 1985. 2363

Lüning, J.: Steinzeitliche Bauern in Deutschland: die Landwirtschaft im Neolithikum, Universitätsforschungen zur prähistorischen Archäologie, 58, Bonn, 2000. 2363

Lynch, J. A., Clark, J. S., and Stocks, B. J.: Charcoal production, dispersal, and deposition from the Fort Providence experimental fire: interpreting fire regimes from charcoal records in boreal forests, Can. J. Forest Res., 34, 1642–1656, 2004a. 2349

Lynch, J. A., Hollis, J. L., and Hu, F. S.: Climatic and landscape controls of the boreal forest fire regime: Holocene records from Alaska, J. Ecol., 92, 477–489, 2004b. 2392, 2393

Mäkipää, R.: Effect of nitrogen input on carbon accumulation of boreal forest soils and ground vegetation, Forest Ecol. Manag., 79, 217–226, 1995. 2382

Malhi, Y., Wood, D., Bakers, T. R., Wright, J., Phillips, O. L., Cochrane, T., Meir, P., Chave, J., Almeida, S., Arroyo, L., Higuchi, N., Killeen, T. J, Laurance, S. G., Laurance, W. F., Lewis, S. L., Monteagudo, A., Neill, D. A., Vargas, P. N., Pitman, N. C. A., Quesada C. A., Salomao, R., Silva, J. N. M., Lezama, A. T, Terborgh, J., Vasquez-Martinez, R., and Vinceti, B.: The regional variation of aboveground live biomass in old-growth Amazonian forests, Glob. Change Biol., 12, 1107–1138, 2006. 2381

Marlon, J. R., Bartlein, P. J., Carcaillet, C., Gavin, D. G., Harrison, S. P., Higuera, P. E., Joos, F., Power, M. J., and Prentice, I. C.: Climate and human influences on global biomass buring over the past two millenia, Nat. Geosci., 1, 697–702, 2008. 2349

GMDD

5, 2347–2443, 2012

SPITFIRE-2: an improved fire module for DGVMs

M. Pfeiffer and J. O. Kaplan

Mason, S. L. R.: Fire and Mesotithic subsistence – managing oaks for acorns in Northwest Europe?, Palaeogeogr. Palaeoclimatol. Palaeoecol., 164, 139–150, 2000. 2398
Mather, A. S.: Forest transition theory and the reforestation of Scotland, Scott. Geogr. J., 120, 83–98, 2004. 2368
Mell, W. E., Charney, J. J., Jenkins, M. A., Cheney, P., and Gould, J.: Numerical simulations of grassland fire behavior from the LANL-FIRETEC and NIST-WFDS models, in: Remote Sensing and Modeling Applications to Wildland Fires; 550 pp. 2012, Springer, Berlin and Heidelberg 2012. 2372
Moorcroft, P. R., Hurtt, G. C., and Pacala, S. W.: A method for scaling vegetation dynamics: the ecosystem demography model (ED), Ecol. Monogr., 71, 557–586, 2001. 2352, 2398
Moreira, A. G.: Effects of fire protection on savanna structure in Central Brazil, J. Biogeogr., 4, 1021–1029, 2000. 2349
Morvan, D., Méradji, S., and Accary, G.: Physical modeling of fire spread in Grasslands, Fire Safety J., 44, 50–61, 2008. 2404
Mouillot, F., Narashima, A., Balkanski, Y., Lamarque, J.-F., and Field, C. B.: Global carbon emissions from biomass burning in the 20th century, Geophys. Res. Lett., 33, L01801, doi:10.1029/2005GL024707, 2006. 2349
Neary, D. G., Ryan, K. C., and DeBano, L. F.: Wildland fire in ecosystems – effects of fire on soil and water, General Technical Report RMRS-GTR-42-volume4, United States Department of Agriculture, Forest Service, Rocky Mountain Research Station, Ogden, UT 84401, 2005. 2349
New, M., Lister, D., Hulme, M., and Makin, I.: A high-resolution data set of surface climate over global land areas, Clim. Res., 21, 1–25, 2002. 2380
Ojima, D. S., Schimel, D. S., Parton, W. J., and Owensby, C. E.: Long- and short-term effects of fire on nitrogen cycling in tallgrass prairie, Biogeochemistry, 24, 67–84, 1994. 2349
Oleson, K. W., M., L. D., Bonan, G. B., Flanner, M. G., Kluzek, E., Lawrence, P. J., Levis, S., Swenson, S. C., Thornton, P. E., Dai, A., Decker, M., Dickinson, R., Feddema, J. J., Heald, C. L., Hoffman, F., Lamarque, J.-F., Mahowald, N., Niu, G.-Y., Qian, T., Randerson, J. T., Running, S., Sakaguchi, K., Slater, A., Stöckli, R., Wang, A., Yang, Z.-L., Zeng, X., and Zeng, X.: Technical Description of version 4.0 of the Community Land Model (CLM), NCAR TECHNICAL NOTE, NCAR/TN-478+STR, Boulder, CO, 80307-3000, 2010. 2352
Otto, J. S. and Anderson, N. E.: Slash-and-burn cultivation in the Highlands South: a problem in comparative agricultural history, Comp. Stud. Soc. Hist., 24, 131–147, 1982. 2368

GMDD
5, 2347–2443, 2012

SPITFIRE-2: an improved fire module for DGVMs

M. Pfeiffer and J. O. Kaplan

Pausas, J. G. and Keeley, J. E.: A burning story: the role of fire in the history of life, BioScience, 59, 593–601, 2009. 2349, 2367

Penner, J. E., Dickinson, R. E., and O'Neill, C. A.: Effects of aerosol from biomass burning on the global radiation budget, Science, 256, 1432–1434, 1992. 2349

Perry, D. A., Hessburg, P. F., Skinner, C. N., Spies, T. A., Stephens, S. L., Taylor, A. H., Franklin, J. F., McComb, B., and Riegel, G.: The ecology of mixed severity fire regimes in Washington, Oregon, and Northern California, Forest Ecol. Manag., 262, 703–717, 2011. 2365

Peterson, D., Wang, J., Ichoku, C., and Remer, L. A.: Effects of lightning and other meteorological factors on fire activity in the North American boreal forest: implications for fire weather forecasting, Atmos. Chem. Phys., 10, 6873–6888, doi:10.5194/acp-10-6873-2010, 2010. 2357, 2360

Peterson, D. L. and Ryan, K. C.: Modeling postfire conifer mortality for long-range planning, Environ. Manage., 10, 797–808, 1986. 2353, 2398

Ping, S.-L., Michaelson, G. J., Jorgenson, M. T., Kimble, J. M., Epstein, H., Romanovsky, V. E., and Walker, D. A.: High stocks of soil organic carbon in the North American Arctic region, Nat. Geosci., 1, 615–619, 2008. 2381, 2382

Power, M. J., Marlon, J. R., Ortiz, N., Bartlein, P. J., Harrison, S., Mayle, F. E., Ballouche, A., Bradshaw, R. H. W., Carcaillet, C., Cordova, C. Mooney, S., Prentice, I. C., Thonicke, K., Tinner, W., Whitlock, C., Zhang, Y., Zhao, Y., Ali, A. A., Anderson, R. S., Beer, R., Behling, H., Briles, C., Brown, K. J., Brunelle, A., Bush, M., Camill, P., Chu, G. Q., Clark, J., Colombaroli, D., Connor, S., Daniau, A.-L., Daniels, M., Dodson, J., Doughty, E., Edwards, M. E., Finsinger, W., Foster, D., Frechette, J., Gaillard, M.-J., Gavin, D. G., Gobet, E., Haberle, S., Hallet, D. J., Higuera, P., Hope, G., Horn, S., Inoue, J., Kaltenrieder, P. , Kennedy, L., Kong, Z. C., Larsen, C., Long, C. J., Lynch, J., Lynch, E. A., McGlone, M., Meeks, S., Mensing, S., Meyer, G., Minckley, T., Mohr, J., Nelson, D. M., New, J., Newnham, R., Noti, R., Oswald, W. , Pierce, J., Richard, P. J. H., Rowe, C., Sanchez Goni, M. F., Shuman, B. N., Takahara, H., Toney, J., Turney, C., Urrego-Sanchez, D. H., Umbanhowar, C., Vergoes, M., Vanniere, B., Vescovi, E., Walsh, M., Wang, X., Williams, N., Wilmshurst, J., and Zhang, J. H.: Changes in fire regimes since the Last Glacial Maximum: an assessment based on a global synthesis and analysis of charcoal data, Clim. Dynam., 30, 887–907, 2008. 2350

GMDD

5, 2347–2443, 2012

SPITFIRE-2: an improved fire module for DGVMs

M. Pfeiffer and J. O. Kaplan

Power, M. J., Marlon, J. R., Bartlein, P. J., and Harrison, S. P.: Fire history and the Global Charcoal Database: a new tool for hypothesis testing and data exploration, Paleogeogr. Palaeoclimatol. Palaeoecol., 291, 52–59, 2010. 2350

Pregitzer, K. S. and Euskirchen, E. S.: Carbon cycling and storage in world forests: biomae patterns related to forest age, Glob. Change Biol., 10, 2052–2077, 2004. 2381, 2382

Prentice, I. C., Kelley, D. I., Foster, P. N., Friedlingstein, P., Harrison, S. P., and Bartlein, P. J.: Modeling fire and the terrestrial carbon balance, Global Biogeochem. Cy., 25, GB3005, doi:10.1029/2010GB003906, 2011. 2354

Pyne, S. J.: Fire in America: a Cultural History of Wildland and Rural Fire, Princeton University Press, Princeton, NJ, 1982. 2349, 2365

Pyne, S. J.: Maintaining focus: an introduction to anthropogenic fire, Chemosphere, 29, 889–911, 1994. 2349, 2363

Pyne, S. J.: World Fire: the Culture of Fire on Earth, University of Washington Press, 384 pp., Seattle, WA, 1997. 2349, 2363, 2399

Rasul, G. and Thapa, G. B.: Shifting cultivation in the mountains of South and Southeast Asia: regional patterns and factors influencing the change, Land Degrad. Dev., 14, 495–508, 2003. 2368

Reinhardt, E. D., Keane, R. E., and Brown, J. K.: First Order Fire Effects Model: FOFEM 4.0, user's guide, General Technical Report INT-GTR-344, United States Department of Agriculture, Forest Service, Intermountain Research Station, Missoula, Montana 59807, 1997. 2351, 2353

Richardson, C. W. and Wright, D. A.: WGEN: A Model for Generating Daily Weather Variables; ARS-8, United States Department of Agriculture, Agricultural Research Service, Springfield, VA 22161, 1984. 2361

Ringeval, B., de Noblet-Ducoudré, N., Ciais, P., Bousquet, P., Prigent, C., Papa, F., and Rossow, W. B.: An attempt to quantify the impact of changes in wetland extent on methane emissions on the seasonal and interannual time scales, Global Biogeochem. Cy., 24, GB2003, doi:10.1029/2008GB003354, 2010. 2390

Ritter, E.: Forests in landscapes – the myth of untouched wilderness, World Forest, 9, 11–27, 2011. 2398

Rius, D., Vannière, B., and Galop, D.: Holocene history of fire, vegetation and land use from the Central Pyrenees (France), Quat. Res., 77, 54–64, 2012. 2350

GMDD

5, 2347–2443, 2012

SPITFIRE-2: an improved fire module for DGVMs

M. Pfeiffer and J. O. Kaplan

Roos, C. I., Sullivan, A. P., and NcNamee, C.: Paleoecological evidence for systematic indigenous burning in the upland southwest, in: The Archaeology of Anthropogenic Environments, 142–171, Southern Illinois University Press, Carbondale, 2010. 2363
Rösch, M., Ehrmann, O., Herrmann, L., Schulz, E., Bogenrieder, A., Goldammer, J. P., Hall, M., Page, H., and Schier, W.: An experimental approach to Neolithic shifting cultivation, Veg. Hist. Archaebot., 11, 143–154, 2002. 2363
Rothermel, R. C.: A mathematical model for predicting fire spread in wildland fuels, USDA Forest Service Research Paper, INT-115, 48, Ogden, UT 84401, 1972. 2351
Rothermel, R. C.: Predicting behavior and size of crown fires in the Northern Rocky Mountains, Research Paper INT-483, United States Department of Agriculture, Forest Service, Intermountain Research Station, Ogden, UT 84401, 1991. 2396
Roxburgh, S. H., Shea, K., and Wilson, J. B.: The intermediate disturbance hypothesis: patch dynamics and mechanisms of species coexistence, Ecology, 85, 359–371, 2004. 2365
Ruddiman, W. F.: The early anthropogenic hypothesis: challenges and responses, Rev. Geophys., 45, 37, RG4001, 1–37, 2006RG000207, 2007. 2349
Ruesch, A. and Gibbs, H. K.: New IPCC Tier-1 Global Biomass Carbon Map for the Year 2000, Tech. rep., Carbon Dioxide Information Analysis Center, Oak Ridge National Laboratory, Oak Ridge, Tennessee, 2008. 2395
Saatchi, S. S., Houghton, R. A., Alves, D., and Nelson, B.: Amazon Basin aboveground live biomass distribution map: 1999–2000, Data Set from Oak Ridge National Laboratory Distributed Active Archive Center, Oak Ridge, Tennessee, USA, 2009. 2381, 2435
Saatchi, S. S., Harris, N. L., Brown, S., Lefsky, M., Mitchard, E. T. A., Salas, W., Zutta, B. R., Buermann, W., Lewis, S. L., Hagen, S., Petrova, S., White, L., Silman, M., and Morel, A.: Benchmark map of forest carbon stocks in tropical regions across three continents, Proc. Natl. Acad. Sci., 1–6, 108, doi:10.1073/pnas.1019576108, 2010. 2395
Sato, H., Itoh, A., and Kohyama, T.: SEIB-DGVM: a new Dynamic Global Vegetation Model using a spatially explicit individual-based approach, Ecol. Model., 200, 279–307, 2007. 2352
Seiler, W. and Crutzen, P. J.: Estimates of gross and net fluxes of carbon between the biosphere and the atmosphere from biomass burning, Climatic Change, 2, 207–247, 1980. 2368
Shu-ren, Y.: Effects of fire disturbance on forest hydrology, J. Forest. Res., 14, 331–334, 2003. 2349
Sigaut, F.: Swidden cultivation in Europe, a question for tropical anthropologists, Soc. Sci. Inform., 18, 679–694, 1979. 2368

GMDD
5, 2347–2443, 2012

Sitch, S., Smith, B., Prentice, I. C., Arneth, A., Bondeau, A., Cramer, W., Kaplan, J. O., Levis, S., Lucht, W., Sykes, M. T., Thonicke, K., and Venevsky, S.: Evaluation of ecosystem dynamics, plant geography and terrestrial carbon cycling in the LPJ dynamic global vegetation model, Glob. Change Biol., 9, 161–185, 2003. 2352, 2371

Skinner, C. N. and Chang, C.-R.: Fire regimes, past and present, Sierra Nevada ecosystem project: final report to congress, II, Assessments and Scientific Basis for Management Options, Sierra Nevada Ecosystem Project: Final report to Congress, II, Assessments and Scientific Basis for Management Options, Wildland Resources Center Report, 37, Centers for Water and Wildland Resources, University of California, Davis, 1041–1069, 1996. 2367

Smith, B., Prentice, I. C., and Sykes, M. T.: Representation of vegetation dynamics in the modelling of terrestrial ecosystems: comparing two contrasting approaches within European climate space, Global Ecol. Biogeogr., 10, 621–637, 2001. 2398

Smittinand, T., Ratanakhon, S., Banijbatana, D., Komkris, T., Zinke, P. J., Hinton, P., Keen, F. B., Charley, J. L., McGarity, J. W., and Pelzer, K. J.: Farmers in the Forest. Economic Development and Marginal Agriculture in Northern Thailand, University of Hawai'i Press, Honolulu, HI 96822, 1986. 2368

Sohngen, B. L. and Haynes, R. W.: The potential for increasing carbon storage in United States unreserved timberlands by reducing forest fire frequency: an economic and ecological analysis, Climatic Change, 35, 179–197, 1997. 2349

Stewart, O. C., Lewis, H. T., and Anderson, K.: Forgotten Fires: Native Americans and the Transient Wilderness, University of Oklahoma Press, 364 pp., Norman, OK 73069, 2002. 2349, 2363

Stocks, B. J.: The extent and impact of forest fires in northern circumpolar countries, in: Global Biomass Burning: Atmospheric, Climatic, and Biospheric Implications, MIT Press, Cambridge, Massachusetts, USA, 197–202, 1991. 2349

Stocks, B. J., Mason, J. A., Todd, J. B., Bosch, E. M., Wotton, B. M., Amiro, B. D., Flannigan, M. D., Hirsch, K. G., Logan, K. A., Martell, D. L., and Skinner, W. R.: Large forest fires in Canada, 1959–1997, J. Geophys. Res., 108, 8149, doi:10.1029/2001JD000484, 2003. 2357

Sundarambal, P., Balasubramanian, R., Tkalich, P., and He, J.: Impact of biomass burning on ocean water quality in Southeast Asia through atmospheric deposition: field observations, Atmos. Chem. Phys., 10, 11323–11336, doi:10.5194/acp-10-11323-2010, 2010. 2349

GMDD
5, 2347–2443, 2012

Tachajapong, W., Lozano, J., Mahalingam, S., Zhou, X., and Weise, D. R.: An investigation of crown fuel bulk density effects on the dynamics of crown fire initiation in shrublands, Combust. Sci. Technol., 180, 593–615, 2008. 2396

Thonicke, K., Venevsky, S., Sitch, S., and Cramer, W.: The role of fire disturbance for global vegetation dynamics: coupling fire into a Dynamic Global Vegetation Model, Global Ecol. Biogeogr., 10, 661–677, 2001. 2352

Thonicke, K., Spessa, A., Prentice, I. C., Harrison, S. P., Dong, L., and Carmona-Moreno, C.: The influence of vegetation, fire spread and fire behaviour on biomass burning and trace gas emissions: results from a process-based model, Biogeosciences, 7, 1991–2011, doi:10.5194/bg-7-1991-2010, 2010. 2353, 2354, 2355, 2356, 2357, 2360, 2365, 2373, 2383, 2396, 2399

Tilman, D., Reich, P., Phillips, H., Menton, M., Patel, A., Vos, E., Peterson, D., and Knops, J.: Fire suppression and ecosystem carbon storage, Ecology, 81, 2680–2685, 2000. 2349

Tinner, W., Conedera, M., Ammann, B., and Lotter, A. F.: Fire ecology north and south of the Alps since the last ice age, Holocene, 15, 1214–1226, 2005. 2363

Tinner, W., Hu, F. S., Beer, R., Kaltenrieder, P., Scheurer, B., and Krähenbühl, U.: Postglacial vegetational and fire history: pollen, plant macrofossil and charcoal records from two Alaskan lakes, Veg. Hist. Archaebot., 15, 279–293, doi:10.1007/s00334-006-0052-z, 2006. 2392, 2393

Turetsky, M., Wieder, K., Halsey, L., and Vitt, D.: Current disturbance and the diminishing peatland carbon sink, Geophys. Res. Lett., 29, 1526, 11, 279–293, doi:10.1007/s00334-006-0052-z, 2002. 2383

Unruh, J. D., Treacy, J. M., Alcorn, J. B., and Flores Paitán, S.: Swidden-fallow agroforestry in the Peruvian Amazon, in: The New York Botanical Garden, edited by: Denevan, W. M. and Padoch, C., Bronx, New York, USA, Adv. Econ. Bot., 5, 107 pp., ISBN O 89327-325-2, 1987. 2368

Van Reuler, H. and Janssen, B. H.: Comparison of the fertilizing effects of ash from burnt secondary vegetation and of mineral fertilizers on upland rice in South-West Cote d'Ivoire, Fert. Res., 45, 1–11, 1996. 2368

Van Wagner, C. E.: Conditions for the start and spread of crown fires, Can. J. Forest Res., 7, 23–34, 1977. 2396

GMDD

5, 2347–2443, 2012

SPITFIRE-2: an improved fire module for DGVMs

M. Pfeiffer and J. O. Kaplan

Vannière, B., Colombaroli, D., Chapron, E., Leroux, A., Tinner, W., and Magny, M.: Climate versus human-driven fire regimes in Mediterranean landscapes: the Holocene record of Lago dell'Accesa (Tuscany, Italy), Quat. Sci. Rev., 27, 1181–1196, 2008. 2350

Venevsky, S., Thonicke, K., Sitch, S., and Cramer, W.: Simulating fire regimes in human-dominated ecosystems: Iberian Peninsula case study, Glob. Change Biol., 8, 984–998, 2002. 2352

Virts, K. S., Wallace, J. M., Hutchins, M. L., and Holzworth, R. H.: A new ground-based, hourly global lightning climatology, B. Am. Meteor. Soc., in review, 2012. 2360

Wan, S., Hui, D., and Luo, Y.: Fire effects on nitrogen pools and dynamics in terrestrial ecosystems: a meta-analysis, Ecol. Appl., 11, 1349–1365, 2001. 2349

Wang, T., Hamann, A., Spittlehouse, D. L., and Murdock, T. Q.: ClimateWNA – high-resolution spatial climate data for Western North America, J. Appl. Meteorol. Climatol., 51, 16–29, 2011. 2380

Wania, R., Ross, I., and Prentice, I. C.: Integrating peatlands and permafrost into a dynamic global vegetation model: 1. evaluation and sensitivity of physical land surface processes, Global Biogeochem. Cy., 23, GB3014, doi:10.1029/2008GB003412, 2009. 2390

West, P. C., Gibbs, H. K., Monfreda, C., Wagner, J., Barford, C. C., Carpenter, S. R., and Foley, J. A.: Trading carbon for food: global comparison of carbon stocks vs. crop yields on agricultural land, Proc. Natl. Acad. Sci., 107, 19645–19648, 2010. 2395

Whitlock, C. and Larsen, C.: Charcoal as a fire proxy, Dev. Paleoenviron. Res., 3, 75–97, 2002. 2349

Williams, G. W.: Introduction to Aboriginal fire use in North America, Fire Manag. Today, 60, 3, 8–12, 2000. 2349, 2363

Williams, M.: Deforesting the Earth: From Prehistory to Global Crisis, University of Chicago Press, Chicago, IL, 2002. 2368

Wincen, R.: The pastoral industry of Cape York Peninsula, Cape York Peninsula Land Use Talkback, Brisbane, 4, 8–9, 1993. 2364

Woodward, F. I. and Lomas, M. R.: Vegetation dynamics – simulating responses to climatic change, Biol. Rev., 79, 643–670, 2004. 2352

Wylie, D., Jackson, D. L., Menzel, W. P., and Bates, J. J.: Trends in global cloud cover in two decades of HIRS observations, J. Climate, 18, 3021–3031, 2005. 2380

Zeng, N., Mariotti, A., and Wetzel, P.: Terrestrial mechanisms of interannual CO_2 variability, Global Biogeochem. Cy., 19, doi:10.1029/2004GB002273, 2005. 2352

GMDD

5, 2347–2443, 2012

Table 1. Explanation of variable and parameter abbreviations.

variable	variable explanation	variable unit
l_m	monthly number of lightning flashes	(grid cell^{-1} month^{-1})
LISOTD$_m$	monthly number of lightning flashes from LIS/OTD data set	(grid cell^{-1} month^{-1})
CAPE$_{anom}$	normalized CAPE anomaly of given month	(grid cell^{-1} month^{-1})
ieff$_{avg}$	average ignition efficiency	(–)
ieff$_{pft}$	PFT-specific ignition efficiency	(–)
fpc$_{grid}$	foliar projected cover fraction of PFT on grid cell	(–)
ieff$_{bf}$	ignition efficiency determined by burned area fraction of grid cell	(–)
ieff	overall ignition efficiency	(–)
burnedf	cumulative fraction of total grid cell area burned during the year	(–)
FDI	Fire danger index	(–)
rf	risk factor	(–)
ig$_p$	number of ignitions per fire-lighting person	(person^{-1} day^{-1})
D_{walk}	average walking distance per fire-lighting person	(m)
W_f	width of a single fire (shorter axis of burn ellipse)	(m)
DT	distance travelled by fire (length of major axis of burn ellipse)	(m)
LB	length-to-breadth ratio of the burn ellipse	(–)
Ab$_{pd}$	potential area that one person can burn	(ha d^{-1})
$\bar{a}_f$	average size of a single fire on a given day	(ha)
target$_{d,group}$	daily burning target	(ha d^{-1} group^{-1})
target$_{y,group}$	annual burning target	(ha yr^{-1} group^{-1})
bf$_{20}$	20-yr running mean of annual burned area fraction	(–)
n_{hig}	number of human-caused ignitions	(d^{-1})
people	10 % of all people within a given lifestyle group	(–)
ac_area	average contiguous area size of patches with natural veget.	(ha)
f_{nat}	fraction of gridcell covered with natural vegetation	(–)
A_{gc}	grid cell area	(ha)
$\rho_{livegrass}$	fuel bulk density of live grass	(kg m^{-3})
GDD$_{20}$	20-yr-average number of growing degree days	(°C)
U_f	mean wind speed	(m min^{-1})
ROSf$_{sg}$	forward rate of spread of fire in herbaceous fuels	(m min^{-1})
rm	relative moisture of the fuel relative to its moisture of extinction	(–)
ω_{nl}	mean relative moisture content of 1 h fuel class and live grass	(–)
me$_{nl}$	mass-weighted average moisture of extinction for live grass and 1 h fuel	(–)
$\omega(1)$	moisture content of the 1 h fuel class	(–)
woi(1)	dead fuel mass in 1 h fuel class	(g m^{-2})
ω_{lg}	relative moisture content of live grass	(–)

GMDD
5, 2347–2443, 2012

SPITFIRE-2: an improved fire module for DGVMs

M. Pfeiffer and
J. O. Kaplan

Table 1. Continued.

variable	variable explanation	variable unit
$w_{lifegrass}$	mass of live grass	(gm^{-2})
$w_{finefuel}$	sum of live grass mass and 1 h dead fuel class	(gm^{-2})
SOM_{surf}	mass of organic matter in the O-horizon	(gm^{-2})
$me_{fc}(1)$	moisture of extinction for 1 h fuel size class (0.404)	(–)
me_{lf}	moisture of extinction for live grass fuels (0.2)	(–)
ω_o	relative daily litter moisture	(–)
me_{avg}	mass-weighted average moisture of extinction over all fuels	(–)
α	drying parameter for the fuel size classes (1.5×10^{-3}, 8.13×10^{-5}, 2.22×10^{-5}, 1.5×10^{-6})	($^{\circ}C^{-2}$)
wn	total fuel (live mass of herbaceous, plus dead mass including all PFTs and fuel size classes 1–3)	(gm^{-2})
woi(1:3)	1-, 10- and 100-h dead fuel mass summed across all PFTs	(gm^{-2})
wo	total mass of dead fuel summed across the first three fuel classes and all PFTs	(gm^{-2})
wtot	total dead fuel mass within the first three fuel size classes, plus mass of the live grass	(gm^{-2})
me_{fc}	moisture of extinction for the four fuel size classes (0.404, 0.487, 0.525, 0.5440)	(–)
me_{lf}	moisture of extinction for live grass/herbaceous fuels (0.2)	(–)
$ROSf_{sw}$	surface forward rate of spread in woody fuels	($mmin^{-1}$)
$ROSf_{sg}$	surface forward rate of spread in herbaceous fuels	($mmin^{-1}$)
treecover	fraction of grid cell area covered by tree pfts	(–)
grasscover	fraction of grid cell covered by grass pfts	(–)
$livefuel_{1hr}$	1 h live fuel summed across all tree PFTs	(gm^{-2})
ROSf	Rate of forward spread	($mmin^{-1}$)
$ROSf_s$	Rate of surface forward spread	($mmin^{-1}$)
$ROSf_c$	Rate of crown forward spread	($mmin^{-1}$)
slf	slope factor	(–)
γ	slope angle	(degrees)
$fires_d$	number of fires on current day	(d^{-1})
$fires_{d-1}$	number of fires on previous day	(d^{-1})
$fires_{new}$	newly ignited fires on current day	(d^{-1})

GMDD
5, 2347–2443, 2012

Table 2. Observed and simulated mean (standard deviation) area burned and burned percent of total ecoregion area over the time period 1986–2010 by ecoregion.

	IB	AT	ART	BTA	BTU	CR	AM
observation (km^2)	4834 (6285)	138 (281)	91 (109)	86 (146)	48 (104)	13 (38)	1 (5)
observation (% area)	0.96 (1.25)	0.04 (0.08)	0.04 (0.05)	0.03 (0.06)	0.05 (0.10)	0.01 (0.02)	0.00 (0.00)
simulated (km^2)	4736 (5654)	680 (1782)	134 (393)	22 (70)	15 (33)	10 (47)	0 (0)
simulated (% area)	0.94 (1.13)	0.19 (0.51)	0.06 (0.19)	0.01 (0.03)	0.01 (0.03)	0.01 (0.03)	0.00 (0.00)

GMDD
5, 2347–2443, 2012

Table A1. PFT-specific parameters. TrBE = tropical broadleaf evergreen, TrBR = tropical broadleaf raingreen, TeNE = temperate needleleaf evergreen, TeBE = temperate broadleaf evergreen, TeBS = temperate broadleaf summergreen, BoNE = boreal needleleaf evergreen, BoS = boreal summergreen, C_3gr = C_3 perennial grass, C_4gr = C_4 perennial grass.

	TrBE	TrBR	TeNE	TeBE	TeBS	BoNE	BoS	C_3gr	C_4gr
F	0.160	0.350	0.094	0.070	0.094	0.094	0.094	–	–
CLf	0.33	0.10	0.33	0.33	0.33	0.33	0.33	–	–
RCK	0.4	0.4	0.1	0.1	0.75	0.1	0.1	–	–
$ieff_{pft}$	0.05	0.40	0.10	0.10	0.50	0.44	0.44	0.50	0.50
$emfact_{CO2}$	1580	1664	1568	1568	1568	1568	1568	106	1664
$emfact_{CO}$	103	63	106	106	106	106	106	106	63
$emfact_{CH4}$	6.8	2.2	4.8	4.8	4.8	4.8	4.8	4.8	2.2
$emfact_{VOC}$	8.1	3.4	5.7	5.7	5.7	5.7	5.7	5.7	3.4
$emfact_{TPM}$	8.5	8.5	17.6	17.6	17.6	17.6	17.6	17.6	8.5
$emfact_{NOx}$	2.0	2.54	3.24	3.24	3.24	3.24	3.24	3.24	2.54
$\rho_{b,PFT}$	15	15	15	15	15	15	15	$\rho_{livegrass}$	$\rho_{livegrass}$

GMDD
5, 2347–2443, 2012

Table A2. Explanation of variable and parameter abbreviations.

variable	variable explanation	variable unit
df(PFT,class)	dead fuel load per PFT in 1-, 10-, 100-, and 1000-h fuel class	($gDM\,m^{-2}$)
lf(PFT,class)	live fuel load per PFT in 1-, 10-, 100-, and 1000-h fuel class	($gDM\,m^{-2}$)
laf(PFT)	fast-decomposing aboveground litter, per PFT	($gC\,m^{-2}$)
las(PFT)	slow-decomposing aboveground litter, per PFT	($gC\,m^{-2}$)
lbg(PFT)	belowground litter, per PFT	($gC\,m^{-2}$)
$N_{ind(PFT)}$	individual density, per PFT	(m^{-2})
$lm_{ind(PFT)}$	leaf mass of the average individual	($gC\,ind^{-1}$)
$sm_{ind(PFT)}$	sapwood mass of the average individual	($gC\,ind^{-1}$)
$hm_{ind(PFT)}$	lheartwood mass of the average individual	($gC\,ind^{-1}$)
$rm_{ind(PFT)}$	root mass of the average individual	($gC\,ind^{-1}$)
woi(class)	1-, 10-, 100- and 1000-h dead fuel mass summed across all PFTs	($g\,m^{-2}$)
ω_{s1}	relative moisture content of top soil layer	(–)
α_{lg}	drying parameter for live grass fuel	($°C^{-2}$)
NI	Nesterov fuel dryness index	($°C^{-2}$)
rel_m	relative moisture content of the fuel relative to its moisture of extinction	(–)
ρ_b	fuel bulk density	($kg\,m^{-3}$)
σ	surface-to-volume ratio of the fuel	($cm^2\,cm^{-3}$)
$\rho_{PFT(PFT)}$	bulk density of dead fuel per PFT, mass-weighted over first 3 fuel size classes	($kg\,m^{-3}$)
pftdeadfuel(PFT)	mass of dead fuel per PFT summed over the first 3 fuel size classes	($g\,m^{-2}$)
β	packing ratio (fuel bulk density/oven dry particle density)	(–)
ρ_p	oven-dry particle density: 513	($kg\,m^{-3}$)
β_{op}	optimum packing ratio	(–)
p_{ratio}	ratio of packing ratio to optimum packing ratio	(–)
Γ'_{max}	maximum reaction velocity	(min^{-1})
Γ'	optimum reaction velocity	(min^{-1})
ν_M	moisture dampening coefficient	(–)
IR	reaction intensity	($kJ\,m^{-2}\,min^{-1}$)
ν_s	mineral dampening coefficient, 0.41739	(–)
h	heat content of fuel: 18	($kJ\,g^{-1}$)
ξ	ratio of propagating flux to reaction intensity	(–)
Φ_w	wind coefficient	(–)
ϵ	effective heating number	(–)

GMDD
5, 2347–2443, 2012

Table A2. Continued.

variable	variable explanation	variable unit
Q_{ig}	heat of pre-ignition	($kJ\,kg^{-1}$)
$ROSb_s$	rate of backward surface spread	($m\,min^{-1}$)
LB_{tree}	lenght-to-breadth ratio of burn ellipse with tree cover	(–)
LB_{grass}	lenght-to-breadth ratio of burn ellipse with grass cover	(–)
t_{fire}	fire duration	(min)
CF_{lg}	live grass fraction consumed by fire	(–)
CF(class)	fractional consumption of dead fuel, per fuel class	(–)
ω(class)	moisture content, per fuel class	(–)
FC(class)	amount of dead fuel consumed	$g\,m^{-2}$
ST	mineral fraction of total vegetation mass, 0.055	(–)
$I_{surface}$	surface fire line intensity	($kW\,m^{-1}$)
P_{mCK}(PFT)	probability of mortality due to crown damage	(–)
RCK(PFT)	PFT-specific crown damage parameter	(–)
CK(PFT)	crown scorch fraction	(–)
dphen(PFT)	leaf phenology status, per PFT	(–)
SH(PFT)	scorch height	(m)
height(PFT)	tree height	(m)
CL(PFT)	crown lenght of woody PFTs	(m)
F(PFT)	scorch height parameter	(–)
$BB_{dead(PFT,1:5)}$	biomass burned from dead fuel by PFT and fuel type	($g\,m^{-2}$)
$BB_{live(PFT,1:3)}$	biomass burned from live fuel by PFT and fuel type	($g\,m^{-2}$)
AB_{frac}	fractional area burned on the grid cell	(d^{-1})
$ann_{kill(PFT)}$	annual total probability of mortality	(–)
$N_{ind\text{-}kill(PFT)}$	fraction of PFT killed by fire	(–)
BB_{tot}	total C-emissions from burning across all PFTs	($gC\,m^{-2}$)
$BB_{pft(PFT)}$	total burned biomass, per PFT	(kg dry matter m^{-2})
$acflux_{fire}$	annual C-flux fom biomass burning	($g\,m^{-2}$)
Mx(spec)	trace gas emissions, per species (CO_2, CO, CH_4, VOC, TPM, NO_x)	($gx\,m^{-2}$)
aMx(spec)	annual trace gas emissions, per species	($gx\,m^{-2}$)

GMDD
5, 2347–2443, 2012

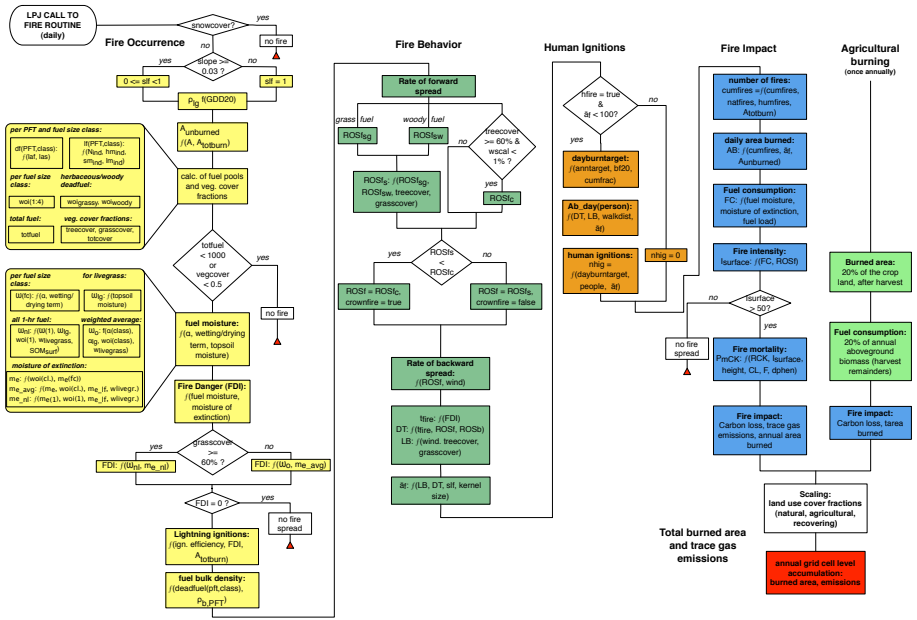

Fig. 1. Flowchart of SPITFIRE-2.

GMDD
5, 2347–2443, 2012

SPITFIRE-2: an improved fire module for DGVMs

M. Pfeiffer and J. O. Kaplan

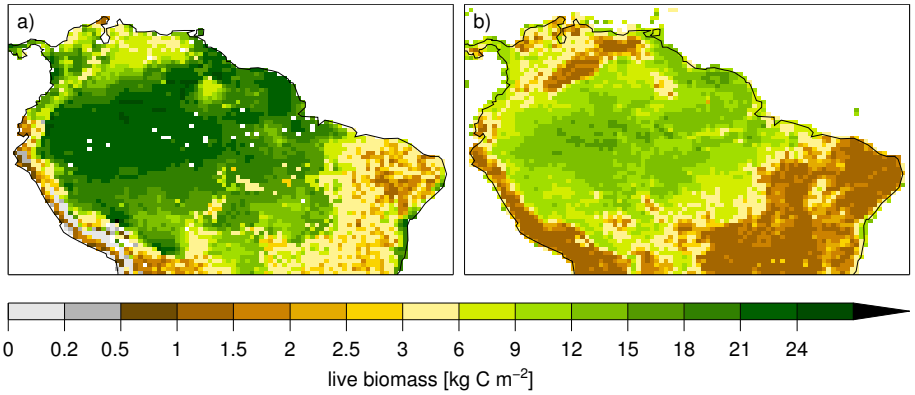

Fig. 2. Simulated aboveground C-storage in living biomass **(a)** after corrections to maximum establishment rate and maximum crown diameter in LPJ compared to aboveground live biomass values values derived from Saatchi et al. (2009) **(b)**.

GMDD
5, 2347–2443, 2012

SPITFIRE-2: an improved fire module for DGVMs

M. Pfeiffer and
J. O. Kaplan

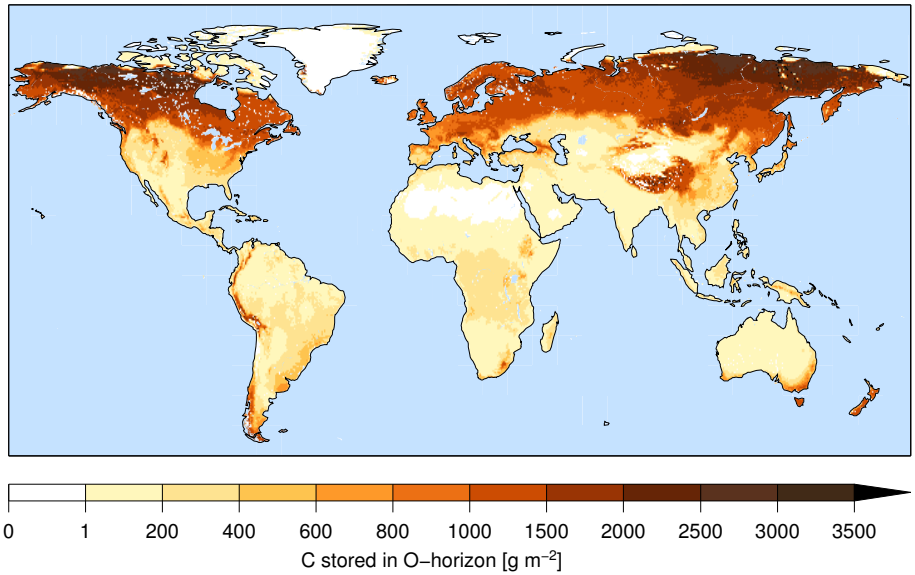

Fig. 3. Simulated C-storage in the organic topsoil layer (O-horizon) newly implemented in LPJ.

GMDD
5, 2347–2443, 2012

SPITFIRE-2: an improved fire module for DGVMs

M. Pfeiffer and
J. O. Kaplan

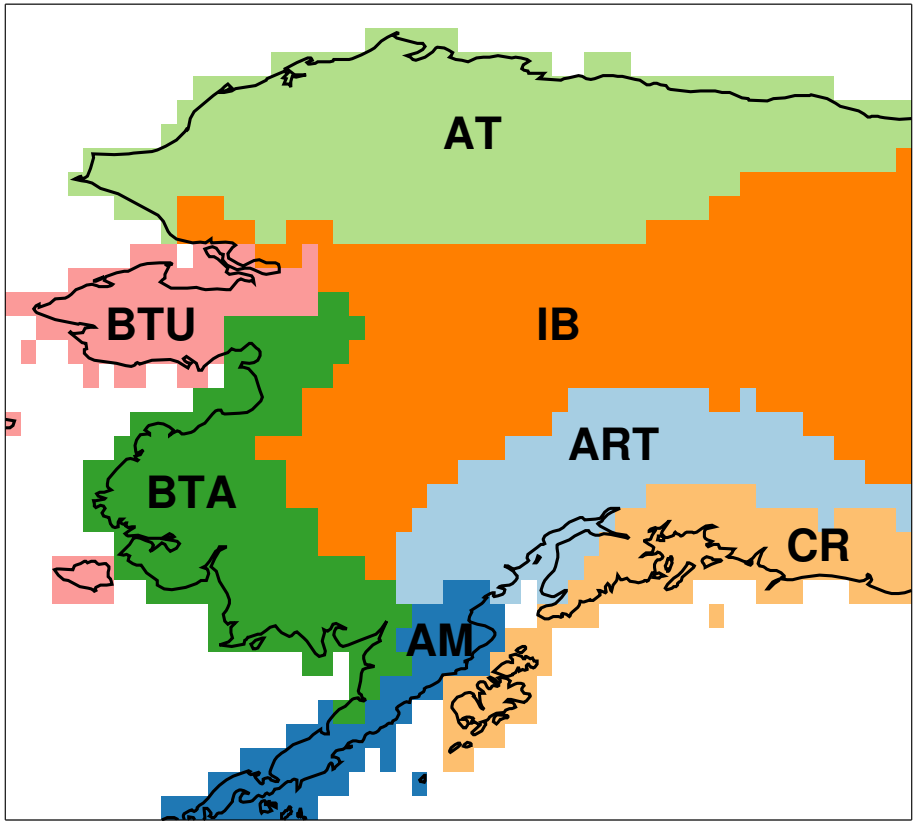

Fig. 4. Alaska ecoregions following the scheme used by the Alaska Fire Service. IB = Intermontane Boreal; AT = Arctic Tundra; ART = Alaska Range Transition; BTA = Bering Taiga; BTU = Bering Tundra; CR = Coastal Rainforest; AM = Aleutian Meadows.

GMDD
5, 2347–2443, 2012

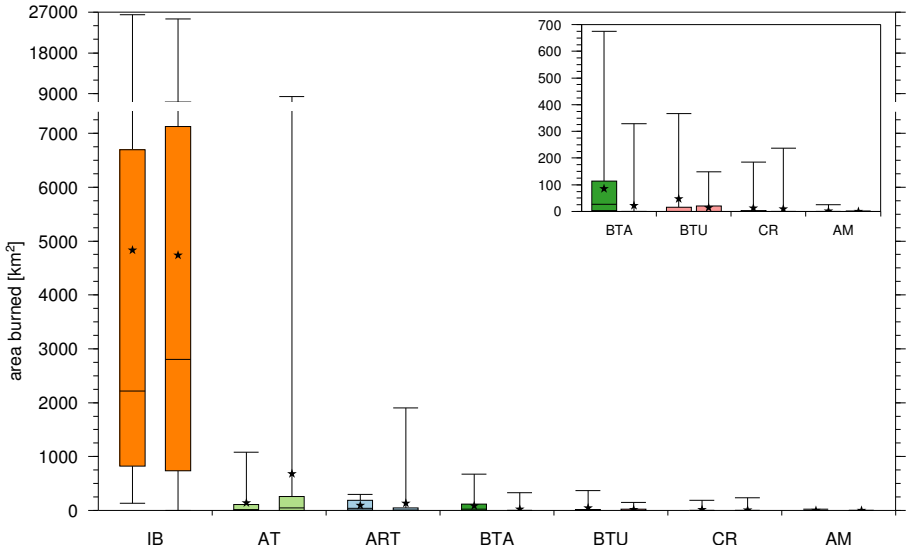

Fig. 5. Boxplots showing the observed (left boxplot) and simulated (right boxplot) minimum, maximum, median and quartiles of area burned between 1986 and 2010 for each of the seven ecoregions. Black stars indicate the statistical mean value.

GMDD
5, 2347–2443, 2012

SPITFIRE-2: an improved fire module for DGVMs

M. Pfeiffer and
J. O. Kaplan

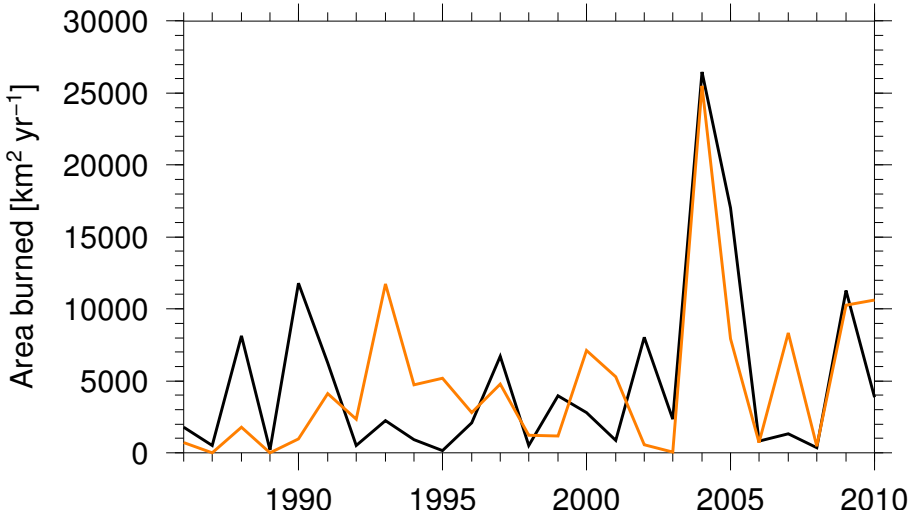

Fig. 6. Simulated (orange) and observed (black) time series of total annual area burned in ecoregion IB between 1986 and 2010.

GMDD
5, 2347–2443, 2012

SPITFIRE-2: an improved fire module for DGVMs

M. Pfeiffer and
J. O. Kaplan

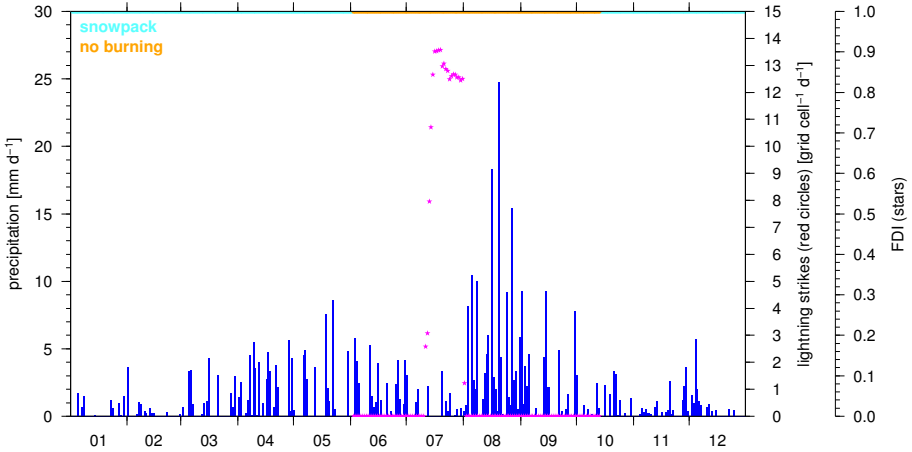

Fig. 7. Typical daily diagnostics for a grid pixel located in ecoregion BTA, showing the daily amount of precipitation (blue bars), FDI (pink stars), lightning strikes (red circles), duration of snowcover (turquoise line at top of panel) and the snow-free time potentially available for burning (yellow line at top of panel). The shown year had a short dry period in Juli with FDI values high enough for burning, but no lightning strike that potentially could have started a fire occurred during this year.

GMDD
5, 2347–2443, 2012

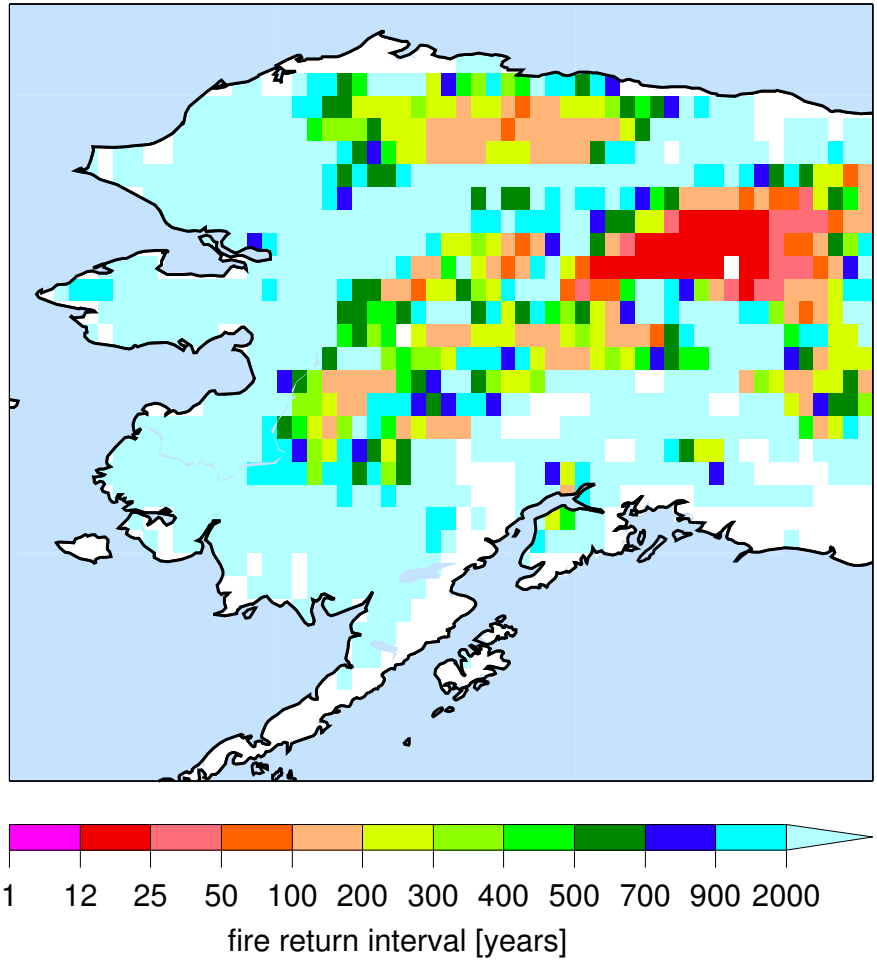

Fig. 8. Simulated fire return intervals in Alaska for a 1000-yr run with detrended 20th century climate.

GMDD
5, 2347–2443, 2012

SPITFIRE-2: an improved fire module for DGVMs

M. Pfeiffer and
J. O. Kaplan

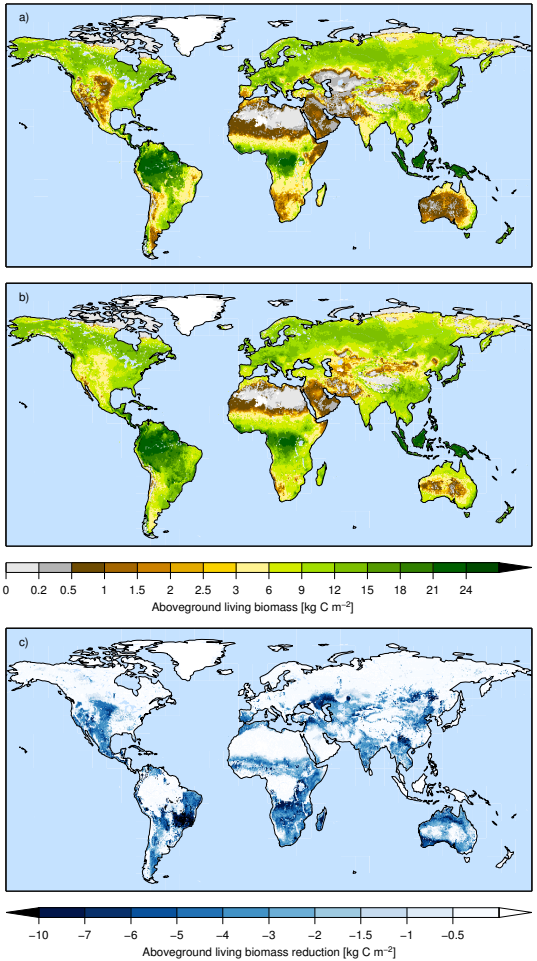

Fig. 9. Simulated biomass C: **(a)** human absence, lightning fires; **(b)** human absence, no fire; **(c)** reduction in biomass C between **(a)** and **(b)**.

GMDD
5, 2347–2443, 2012

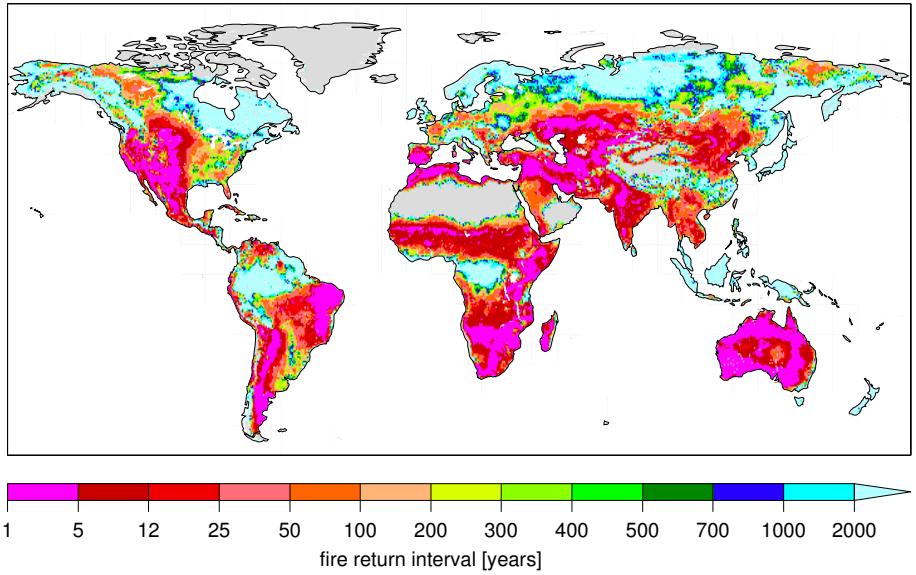

Fig. 10. Simulated global fire return intervals for a model run over a time period of 1000 yr using the detrended 20th century reanalysis and LIS/OTD-derived lightning climatology.

GMDD
5, 2347–2443, 2012

SPITFIRE-2: an improved fire module for DGVMs

M. Pfeiffer and
J. O. Kaplan